Weather Modification Impacts and Forecasting of Streamflow

Final Report

May 1, 2010

USGS-WWDC Water Research Program

Glenn Tootle (PI)[1]

Tom Piechota (Co-PI)[2]

Cody Moser (Graduate Research Assistant)[1]

Ty Soukup (Graduate Research Assistant)[1]

Oubeid Aziz (Graduate Research Assistant)[1]

Haroon Stephen (Post-Doctoral Research Assistant)[2]

[1]University of Wyoming
Department of Civil and Architectural Engineering
1000 E. Univ. Ave.
Dept. 3295
Laramie, WY 82071-2000
tootleg@uwyo.edu
307-766-3299

[2]University of Nevada, Las Vegas
Department of Civil and Environmental Engineering
Box 451087
FDH 516
Las Vegas, NV 89154-1087
thomas.piechota@unlv.edu
702-895-4412

Executive Summary and Research Results

On behalf of the graduate research assistants (Cody Moser, Ty Soukup and Oubeid Aziz), post-doctoral research assistant (Haroon Stephen), Co-PI (Tom Piechota) and the PI (Glenn Tootle), we hereby submit our final report *Weather Modification Impacts and Forecasting of Streamflow*. The research team would also like to acknowledge Shaun Wulff (UW Department of Statistics) for his assistance.

The scientific objectives of the proposed three-year research project were to:

1. Identify and evaluate snowpack, unimpaired streamflow, soil moisture and air temperature datasets in weather modification target areas within the state of Wyoming. *The North Platte River Basin was selected given the weather modification efforts in the basin. Chapter One and Chapter Two of the final report evaluated and utilized datasets in this basin.*
2. Examine relationships between snowpack and streamflow, including the impacts from the previous Fall season soil moisture (antecedent moisture conditions) and following Spring-Summer season air temperature on resulting streamflow from snowpack. This includes determining the optimum (i.e., highest correlation) relationships (period and lag time) between snowpack and streamflow. *Chapter One evaluated the relationships between snowpack, streamflow and antecedent soil moisture in the North Platte River Basin and determined optimum relationships. This included which season and the lag between the predictor and predictand.*
3. Utilizing the optimum relationships, develop statistically based models (regression) for snowpack and resulting streamflow and apply the models to quantify streamflow increase due to snowpack increase as a result of weather modification. *Chapter One developed regression equations, relating snowpack to streamflow, in the North Platte River Basin. These regression equations can be utilized to estimate increases in streamflow based on snowpack increases due to weather modification. At the time of this final report, NCAR has not provided estimates for increased snowpack. Chapter One was the basis of Cody Moser's UW Department of Civil Engineering thesis and was published in the below referenced ASCE EWRI proceedings.*
4. Utilizing relationships between snowpack and streamflow, evaluate statistically based models, including regression and non-parametric approaches, and develop forecasts of streamflow including exceedance probability, forecast skill and uncertainties. *Chapter Two of the final report evaluated long lead-time forecasts of streamflow in the North Platte River Basin, using climate (Sea Surface Temperatures and 500mb pressures). A non-parametric (exceedance probability) streamflow forecast was developed for several streamflow stations in the North Platte River Basin. Chapter Two was the basis of Ty Soukup's UW Department of Civil Engineering thesis and was published in the below referenced Journal of Hydrology.*

The research provided outstanding training and support for the above mentioned graduate students. All three graduate students have completed their master's degree. Ty Soukup is currently employed at Tri Hydro in Laramie, Wyoming while Cody Moser and Oubeid Aziz are currently PhD students at the University of Tennessee.

The results of the research have been published in a conference proceedings and a peer-reviewed journal:

Moser, C., T. Soukup, G. Tootle and T. Piechota, 2008. An Expert System Approach to Improve Streamflow Forecasting in the North Platte River Basin, Wyoming, USA. Proceedings of the *ASCE World Water & Environmental Resources Congress 2008*, May 11-17, 2008, Honolulu, HI.

Soukup, T., O., Aziz, G. Tootle, S. Wulff and T. Piechota, 2009. Incorporating Climate into a Long Lead-Time Non-parametric Streamflow Forecast. *Journal of Hydrology*, 368(2009), 131-142.

In addition to numerous local presentations including the WWDC/WWDO Weather Modification Technical Advisory Committee meetings, the research was presented at the 2008 ASCE EWRI Conference in Honolulu, HI.

The results of the research made several contributions including:

- As expected, there are strong relationships between snowpack (Snow Water Equivalent) and streamflow in the North Platte River Basin. However, the inclusion of Antecedent Soil Moisture resulted in slight improvement in streamflow forecasting skill in the basin and should be considered in future forecasts.
- The use of Sea Surface Temperatures and 500mb pressures resulted in the ability to provide a skillful long lead-time (three to six months) forecast of streamflow in the North Platte River Basin. The identification of these climatic teleconnections may provide important information prior to the winter season during weather modification operations.

Table of Contents

CHAPTER 1 - Improving Streamflow Forecasts by Incorporating Antecedent Soil Moisture

ABSTRACT

A study of incorporating antecedent (preceding) soil moisture into forecasting streamflow volumes within the North Platte River Basin is presented. By integrating antecedent soil moisture as a predictor to forecast streamflow, processes that determine the amount of streamflow, such as infiltration and runoff can be better accounted for. Current Natural Resource Conservation Service (NRCS) forecasting methods are replicated and a comparison is drawn between current NRCS forecasts and proposed forecasting methods. Current predictors used by the NRCS in regression based streamflow forecasting include precipitation, streamflow persistence (previous season streamflow volume) and snow water equivalent (SWE) from SNOTEL (snow telemetry) sites. Proposed methods include utilizing antecedent soil moisture as a predictor variable in addition to currently used predictors and extending the forecast period of record. By extending the period of record, an expert (decision) system is used to segregate data based on antecedent soil moisture conditions (e.g., dry, wet or normal). Correlation techniques are applied to determine ideal predictors. Principal component analysis and stepwise linear regression is applied to generate streamflow forecasts and numerous statistics are determined to measure forecast skill and check for violation of model assumptions. The results show that, when incorporating antecedent soil moisture, overall model skill improved. More importantly, “poor” forecasts (i.e., years in which the NRCS forecast differed greatly from the observed value) were greatly improved. The research shows the need to increase monitoring and the collection of soil moisture data in mountainous western U.S. watersheds.

INTRODUCTION

Streamflow forecasting is the process of predicting a seasonal volume of water at a specific site (gauge) location at a specific time. Generally, in mountainous regions of the western U.S., the season of interest is the spring-summer season when natural supply levels decrease and demand increases due to seasonal influences. The NRCS, in cooperation with the National Weather Service (NWS), issue water supply forecasts for over 750 points in the western U.S. near the first of the month between January and June each year. These forecasts assist water managers/users for future planning according to the forecasted amount of water available. While these forecasts are produced monthly, this study focuses on forecasting the season of interest, which is the cumulative April-May-June-July streamflow volume.

Water managers operate with a shrinking margin of error, facing increasingly complex and competing demands while trying to retain flexibility to adapt to hydro climatic conditions (Pagano et al. 2004). The primary objective of these forecasts is to minimize risk and uncertainty for water managers, therefore creating more efficient use of a scarce resource. Thorough understanding of forecast performance helps decision makers determine when and how much to rely on forecasts as well as how to respond to expected climatic anomalies (Hartman et al. 2002). Over allocated supplies and increasing demands require the precision management of water. While the NRCS has been forecasting water supplies for close to 70 years, it is evident that the physical and demographic landscapes of the Intermountain West are changing (Tom Pagano, unpublished Snow Survey Centennial Newsletter, September 25, 2006). Hartman et al. (2002)

reveals how streamflow forecasts can be more effectively used if scientists look at the user's perspective.

While the NWS use a comprehensive set of models and hydrologic techniques, NRCS forecasts are produced using statistical approaches such as multiple linear regression models. These regression based forecasts rely on measurements of current snowpack, antecedent streamflow and autumn precipitation (Pagano and Garen 2006). The regression models suggest a relationship between predictor variables (precipitation, snow water equivalent, antecedent streamflow, etc.) and the predictand (streamflow volume of interest). Several techniques were developed by Garen (1992) to significantly improve forecast accuracy when using regression models. These techniques include: (1) basing the regression model only on data known at forecast time (no future data); (2) principal components regression; (3) cross validation; and (4) systematic searching for optimal or near-optimal combinations of variables (Garen 1992). Historical practice in forecasting often included variables in regression equations that described future precipitation amounts. The research of Stedinger et al. (1988), Koch (1990) and Garen (1992) proved that use of future variables (variables that describe future snow accumulation or precipitation) and substitution of averages reduced forecasting accuracy, especially early in the forecasting season. Therefore, research presented here does not use future variables, but only variables known at the time of the forecasting process. Currently, the NRCS combines manual measurements, an ever-expanding network of SNOTEL sites, and powerful advances in information technology and data communication to monitor the pulse of western snowpacks and water supplies (Tom Pagano, unpublished Snow Survey Centennial Newsletter, September 25, 2006). This information is communicated to users through innovative new products.

Prior to developing a forecast model, it is vital to analyze predictors. This includes creating and maintaining an extremely high quality historical dataset, subjected to the most rigorous screening and data quality testing (Pagano et al. 2005). As stated by Garen (1992), "A more robust, accurate and consistent forecasting equation can be obtained by having several sites for the same data type and time in the equation." Currently, the predictors obtained for NRCS streamflow forecast models are obtained from remote sensing data sources. Due to the relative newness of these remote sensing sites, the period of record used by the NRCS to develop a streamflow forecast is relatively short (i.e., limited period of record).

The motivation of this research evolved after a meeting with the NRCS in Portland, Oregon (Tom Pagano, personal conversation, October 22, 2007) regarding the forecasting of streamflow in Upper North Platte River Basin. First, the NRCS stated that "The Upper North Platte River Basin was one of the more challenging regions to forecast in the western U.S." An additional question posed was "Is a there a way to increase forecast skill for years in which current NRCS forecasts result in a 'poor' forecast (i.e., NRCS forecast is much different than actual) while improving overall model skill?" The challenge posed to researchers is to achieve these two objectives (improve overall model skill and improve "poor" year forecasts) while constrained to using current NRCS forecasting methods (principal component stepwise linear regression).

In addition to the traditional predictors (snow water equivalent, precipitation, and antecedent streamflow) currently used in streamflow forecast models, this study proposes the incorporation of National Oceanic and Atmospheric Administration (NOAA) climate division soil moisture data. Although soil moisture data is recorded by enhanced SNOTEL (NRCS) sites, antecedent soil moisture (ASM) is not currently used in coordinated NRCS-NWS streamflow forecasts within the North Platte River Basin. Past research that has incorporated soil moisture as a predictor in streamflow forecasting include Day (1985) and Aubert et al. (2003). In addition to incorporating (adding) ASM as a predictor, this research proposes a novel approach in the development of an expert (decision) system based on ASM. This decision system is based on segregating ASM data into three specific categories: wet, normal, and dry. Each category has its own regression equation, utilizing current NRCS methods (principle component stepwise linear regression). It is important to recognize that the development of an expert (decision) system requires increasing the period of record (i.e., extended period of record) to include data (i.e., manually obtained) prior to the deployment of remote sensing collection tools.

Therefore, the contribution of this research is the identification of a valuable predictor (ASM) and a new framework (decision system based on ASM) for improving poor NRCS streamflow forecasts while maintaining overall model skill in the North Platte River Basin. The results support the need to increase monitoring and the collection of soil moisture data, especially in mountainous western U.S. watersheds in which snowpack is the primary driver of streamflow runoff. The collection of soil moisture data will ultimately provide a useful database to improve streamflow forecasts in these regions.

WATERSHED DESCRIPTION

The North Platte River is a tributary of the Platte River, which is approximately 1,094 kilometers in length. The North Platte River originates in Colorado where it flows north into Wyoming, and then flows east to Nebraska (Figure 1.1). Three major reservoirs in Wyoming along the North Platte River are Seminoe, Pathfinder, and Glendo. Present use and future development of water resources in the North Platte River Basin are controlled by the 1945 Supreme Court Decree for the North Platte River.

The North Platte River watershed is predominately located in mountainous regions of Colorado and Wyoming. Thus, most of the annual streamflow is attributed to melting snowpack that has accumulated during winter and early spring months in mountainous headwater regions. Pagano and Garen (2006) suggest that snowmelt provides approximately 80 percent of the streamflow in the western United States. The delay between the time that snow accumulates and then melts creates the opportunity to generate an estimate of the actual amount of runoff.

DATA

Available datasets used to forecast streamflow include antecedent streamflow (streamflow persistence), snow water equivalent, precipitation and ASM.

Streamflow Data

The data used in this study comes from two streamflow stations (USGS 06620000 and USGS 06625000), which are located the Upper North Platte River Basin. The data can be obtained from the United States Geological Survey (USGS) NWIS website (http://waterdata.usgs.gov/nwis/rt). Each of these stations is recognized as being unimpaired (Wallis et al. 1991) and a current forecast for each station is provided by the NRCS. USGS streamflow station 06620000 is the most upstream (southern) station. The station's elevation is 2,380 m above sea level and has a drainage area of 3,706 square kilometers. USGS station 06625000 is located on a downstream tributary (Encampment River) and is 2,124 meters above sea level with a drainage area of 686 square kilometers. See Figure 1.1 for a detailed location map covering the region of study. The USGS provides daily, monthly, and annual mean streamflow in cubic feet per second (cfs). Total monthly streamflow in cubic meters for April-May-June-July (AMJJ) is calculated using appropriate conversions. Antecedent (January-February) streamflow volume, a commonly used predictor in NRCS forecasts, is also utilized.

Snow Water Equivalent (SWE) Data

The NRCS National Water and Climate Center provides snow water equivalent data (in inches) for the western United States (http://www.wcc.nrcs.usda.gov/snow/). Snow water equivalent data is distinguished into 2 groups: snow course & SNOTEL. Early SWE data (snow course) was recorded manually, and SNOTEL data is published in real-time through use of remote sensing stations. Snow course data in the western U.S. dates as far back as 1906 while SNOTEL data in the North Platte River Basin dates back to the early 1970's depending upon when the digital sensors in the station were installed. Within the North Platte River Basin, there are a total of nine SWE stations that are located within and adjacent to the drainage basin (Figure 1.1). These stations provide accumulated precipitation, snow depth, snow water equivalent, temperature, and soil moisture (for enhanced stations) data. April 1 SWE (converted from inches to centimeters) is used as a predictor in the current research.

Precipitation Data

Current NRCS methods use only precipitation data from SNOTEL sites (limited record). Precipitation data is also available from the Western Regional Climate Center (WRCC) website (http://www.wrcc.dri.edu/) using monthly precipitation totals. One precipitation station has data dating back to the year of interest (1940) for the proposed extended record analysis. This station is located in Steamboat Springs, Colorado and has monthly data dating back to 1908. Average precipitation data was obtained for the Steamboat Springs, Colorado station (converted from inches to centimeters) for the period of October through December of the previous year and January through March of the forecasted year.

Antecedent Soil Moisture Data

Data for soil moisture was obtained from the National Oceanic and Atmospheric Administration (NOAA) website (http://www.cpc.ncep.noaa.gov/soilmst/). NOAA soil moisture data is estimated by a one-layer hydrological model (Huang et al. 1996, van den Dool et al. 2003). The model takes observed precipitation and temperature and calculates soil moisture, evaporation and runoff. A study in eastern Oklahoma resulted in a maximum holding capacity of 760 mm of water using a common porosity of 0.47 which implies a soil column of 1.6 meters. Because this soil moisture is modeled data, there is only one value for the entire climate division. Of the 344 climate divisions in the U.S., one soil moisture dataset is within the North Platte River Basin. This station is located in climate division 10 within the state of Wyoming and the data covers an area of 61.6 square kilometers (Figure 1.1). Accessible monthly soil moisture data is available from 1932 to 2005 (74 years). Average ASM for this station in mm (for the period of October through December of the previous year and January through March of the forecasted year) was obtained. The authors acknowledge that NOAA climate division soil moisture contains many uncertainties. However, the primary hypothesis of this research is that ASM is a useful predictor for streamflow forecasting. Currently, this is the best available dataset that provides an extended period of record. Soil moisture data from enhanced SNOTEL (NRCS) stations is relatively new and dates back only a few years. Due to the lack of record, this data is not used in this study.

FORECAST METHODOLOGY

Limited Record (Current NRCS Methods)

The NRCS has developed a Visual Interactive Prediction and Estimation Routine (VIPER) to forecast streamflow. This forecast application gathers all data in real-time directly from the source. Linked with both historical and real-time data, the hydrologist specifies a list of predictor sites for a specified streamflow gage, the type of analysis desired (principal component stepwise linear regression is the most common NRCS method to forecast streamflow in the North Platte River Basin), and equations are automatically developed and the forecast produced in real-time (Tom Pagano, unpublished Snow Survey Centennial Newsletter, September 25, 2006). Pagano's 2006 newsletter details the methodology used for these forecasts and the current research replicates these methods. This real-time approach is very efficient, but has the disadvantage of using only data that has been recorded by digital sensors (limited period of record). Data of this type varies in relation to when the SNOTEL site was installed. The first of these SNOTEL sites in the North Platte River Basin was established in the early 1970's, which limits the digital data that can be used in producing forecasts. For varying streamflow stations, this period of record varies depending upon the available SNOTEL data. In this study, the forecasted period of record (limited) used by the NRCS for USGS streamflow station 06620000 is 1979-2005 (27 years) while 1983-2005 (23) years is the period of record for USGS 06625000. Within the VIPER interface, various types of streamflow transformations can be applied to improve forecast skill. Transforming streamflow data can be a very valuable tool to increase forecast accuracy, especially when recorded streamflow is non-linear. These transformations include square root, cube root, logarithmic, and natural logarithmic. The type of transformation producing the most accurate forecast (R^2) is chosen. USGS 06620000 is most accurately forecasted using a square root transformation. This process involves transforming the streamflow data, running principal component stepwise regression, and finally transforming the streamflow volume back to the proper scale (in this case cubic meters). USGSS 066250000 is most accurately forecasted when the streamflow data is left untransformed.

Current NRCS Methods Incorporating ASM

The previous NRCS forecast methods for the limited record are now replicated with ASM added as a predictor into the principle component analysis. The same transformation, period of record and predictors are used. Results are then analyzed to determine if the addition of ASM results in an increase in forecast skill.

Extended Record (Applying NRCS Methods)

Extending the period of record (back to approximately 1940) is required to develop an expert (decision) system. By extending the forecast period of record, increased variability in hydrologic predictors (and response) can be accounted for and sufficient data is available to develop an expert system. In this region, streamflow data was first measured in the early 1940's. Therefore, data including precipitation, snow water equivalent, and soil moisture in the North Platte River Basin is also required dating back to the same period. For this analysis, ASM is not included because this evaluation was designed to replicate current NRCS forecast methodology for the extended period of record.

Identifying Predictors (Extended Record)

Predictors are identified for the extended period of record. Seasonal streamflow and SWE correlation values are first analyzed. Next, moving time (10, 20, 25, and 30 years) window correlations between streamflow and SWE is performed, as in Biondi et al. (2004). This ensures that reliable and consistent SWE data sets are used (i.e., stability throughout the record) given the uncertainties (e.g., prolonged equipment malfunction, equipment calibration, human error) in the collection of SWE data for various periods of record. Finally, correlation values between snow course/streamflow and SNOTEL/streamflow are analyzed. This will (or will not) confirm that the relationship between snow course/streamflow is similar to the relationship between SNOTEL/streamflow A minimum difference between snow course/streamflow and SNOTEL/streamflow correlation values is essential because stability throughout the period of record is needed to extend the model back to the early 1940's.

A visual inspection of the streamflow and SWE correlations resulted in the following "rules" for the inclusion of the SWE station as a predictor. First, the overall correlation value between SWE and streamflow must exceed 0.55 to be included as a predictor. Second, if any of the moving time window correlations resulted in a negative value, the SWE station was not included. Finally, the comparison between snowcourse/streamflow and SNOTEL/streamflow correlation values must not differ by more than 0.15 to be included.

Precipitation records dating back to the period of interest are for the most part non-existent in the North Platte River Basin. The only location that precipitation data is available dating back to the early 1940's is in Steamboat Springs, Colorado. The previous "rules" are applied to precipitation and streamflow. Finally, streamflow persistence (JF) is also correlated against AMJJ streamflow. After determining the most appropriate predictor variables to extend the period of record, the same methodology used by NRCS (principal component stepwise linear regression) is performed for the extended period of record.

Applying Current NRCS Methods Incorporating ASM

The next analysis adds ASM as a predictor into the principle component analysis. The forecast timeline is kept consistent and previous predictor variables identified are not changed. Additionally, the same forecast methodology is used. This process determines if incorporation of ASM as a predictor results in improved streamflow forecast skill for the extended period of record.

Expert (Decision) System Incorporating ASM

The last analysis in this research segregates predictor variables (i.e., expert system) based solely on ASM (e.g., wet, dry, normal). This requires performing a simple statistical analysis to determine the average and standard deviation of ASM data for the season and record of interest. Wet years are defined as those whose soil moisture is 1.25 standard deviations (σ) above average, and similarly, dry years are defined as those whose soil moisture is 1.25σ below the overall average. Remaining years are considered normal years. The expert system value of 1.25σ is chosen because it produces higher forecast skill when compared to expert systems that group the data based on 0.75σ and 1σ. Using a standard deviation higher than 1.25 is not investigated since it would result in very few extreme years. After grouping the data into the appropriate categories using ASM conditions (wet, normal, dry), principle component stepwise linear regression is performed individually on the three sets of data (wet, normal, dry). This analysis results in three separate regression equations that are used to forecast streamflow based on ASM conditions.

"Poor" NRCS Forecasts

A "poor" streamflow forecast is one that predicts a streamflow volume that is much different than the actual (observed) volume. For this research, a "poor" forecast is determined by ranking (worst to best) each year and selecting the upper quartile (25%) of worst forecasts and defining them as "poor" forecasts. There are a variety of reasons that lead to "poor" streamflow forecast for a particular year. They include: data unavailability, unexpected precipitation, unforeseen drought conditions, and climate change. Any one of these, or all of them, are possible reasons a "poor" forecast is produced. Implications of "poor" streamflow forecasting include: inefficient management/allocation of water, water managers having little confidence in forecasts, and reduced credibility of the forecaster. The hypothesis of this research is that the incorporation of ASM will reduce the "number" of "poor" forecasts while maintaining overall model skill. The physical basis of this hypothesis is that ground surface conditions (wet, dry, normal) will influence the amount of runoff. Simply put, the same snowpack and precipitation for wet ground surface conditions will produce more runoff than dry ground surface conditions.

Statistical Analysis

In forecasting, problems with intercorrelation arise when predictor variables are highly correlated with other predictor variables. For example, antecedent streamflow correlates highly with precipitation and snow water equivalent. The most satisfactory and statistically rigorous way to deal with intercorrelation, and the method applied in this study, is to use principle component regression (Garen 1992). Principle component regression is a useful technique for addressing multicollinearity problems and can yield better predictors (Khattree and Naik 2000). An important property of the principle components is that they are uncorrelated (Anderson 2003). Thus, there are no problems with multicollinearity. The number of components retained in the equation depends upon how many of the components have statistically significant regression coefficients. It is also necessary to determine which principal components to use in the regression equation (Garen 1992). Garen (1992) used a standard t-test to determine significance of the regression coefficient for the component. A similar method, presented in this study, is the use of forward stepwise linear regression to determine the number of principle components to include in the regression model. Forward stepwise regression determines what predictors explain a significant amount of the variance, starting with the predictor that explains the most variance while adding/removing any predictors that do/do not significantly improve the fit. For this study, a stepwise linear regression F-value of 4 is used. For a two-sided test with alpha=0.05 (95% significance) and sample sizes of 20 or more, the critical value for the standard t-test is close to 2. Squaring this t-value produces a critical partial F-value near 4.

Numerous predictive statistics can be calculated to determine the skill of a principle component regression model. These include the standard error of the regression, R^2, adjusted R^2, the PRESS statistic, and the predicted R^2. The standard error of the regression (S) is used to describe model fit and is equivalent to the square root of the mean squared error. S represents the cumulative distance between the data and the fitted regression line. Thus, a lower value of S indicates better prediction of the response from the fitted regression equation. R^2 is a function of S that is scaled to be between 0 and 1. Thus, R^2 measures the proportion of variation in the response that is accounted for by the predictor variables. A higher R^2 indicates a better fit of the model to the data.

Adjusted R^2 also describes the variation of the response variable due to the relationship between the response variable and one or more predictor variables. The relationship is adjusted based upon the number of predictors in the model. R^2 values will always increase when a new predictor is added to the model. However, adjusted R^2 has an adjustment that prevents the model from appearing better simply due to adding marginally important predictor terms.

It is well known that the prediction ability of the model as measured by the previous criteria can provide an overly optimistic measure of the true forecasting performance (Garen 1992). In order to achieve closer representation of forecasting ability, cross validation procedures are recommended. Cross validation creates a validation series by dropping observations corresponding to the years, creating a regression equation for the remaining observations, and then predicting values for those years that were dropped. The PRESS (prediction sum of squares) statistic is such a measure of the predictive ability of the model. PRESS is based upon a leave-one-out cross-validation in which a single year or observation is removed when fitting the model. As a result, the prediction errors are independent of the predicted value at the removed observation (Garen 1992). For selecting a model when the primary interest is in prediction (forecasting), the model with the smaller PRESS is preferable (Montgomery et al. 2006). The PRESS value is also used to calculate the predicted R^2 statistic, which is a "R^2-like" statistic that reflects the prediction capability of the model (Myers 1990). Thus, predicted R^2 ranges from 0 to 1.0. PRESS is on the same scale as the residual sum of squares (squared units).

Another method to measure forecast skill is the linear error in probability (LEPS) score (Ward and Folland 1991; Potts et al. 1996). The LEPS score was originally developed to assess the position of the forecast and the position of the observed values in the cumulative probability distribution. Potts et al. (1996) describe the advantages of the LEPS score over traditional skill measurements such as root-mean-square error. The LEPS score (S'') and the average skill (SK) are defined in Tootle et al. 2007. A LEPS SK score of greater than +10% is generally considered "good skill". The LEPS SK score has been previously utilized as a measure of skill in streamflow forecast models (Piechota et al. 1998; Piechota and Dracup 1999; Tootle and Piechota 2004).

Statistics are also calculated to check for violation of model assumptions. These include autocorrelation and heterogeneity of variance. The Durbin-Watson statistic is used to check for autocorrelation in residuals. If adjacent observations are correlated (autocorrelation), the regression model will underestimate the standard error of the coefficients. As a result of underestimation, predictors may seem to be more significant than they actually are (Minitab Inc. 2007). To test for positive autocorrelation, the Durbin-Watson statistic (d) is compared to lower (dL) and upper (dU) critical values. If $d < dL$, there is statistical evidence that the error terms are positively autocorrelated. If $d > dU$, there is statistical evidence that the error terms are not positively autocorrelated, and if $dL < d < dU$, the test is inconclusive. Recall, that since the regression model is created using principle components, there are no issues with multicollinearity.

An important assumption of the regression model is that the residual error variance is equal or homogeneous across the observations. This assumption can be checked using a test developed by White (1980). This test evaluates whether or not the variance and the mean of the regression model are correctly specified. Under this hypothesis, the test statistic has a particular chi-square distribution from which the p-value (p_c) can be calculated.

RESULTS

Limited Record

A comparison is made between current NRCS methods and current NRCS methods incorporating ASM as a predictor for the limited period of record. In this study, the forecasted period of record (limited) used by the NRCS for USGS streamflow station 06620000 is 1979-2005 (27 years) while 1983-2005 (23) years is the period of record for USGS 06625000. Table 1.1 shows the numerical measures of skill. A slight increase in skill is achieved for both streamflow stations when incorporating ASM across all of these measures. For example, the R^2 value for USGS streamflow station 06620000 increases from 0.82 to 0.83 after incorporating ASM. USGS streamflow station 06625000 R^2 values are 0.79 using current NRCS methods, and 0.82 after ASM is added as a predictor. The LEPS SK scores for USGS 06620000 are 70.2 without soil moisture and 71.0 incorporating soil moisture. LEPS SK scores are 65.4 (without ASM) and 67.6 (with ASM) for USGS 06625000. While the authors acknowledge the increase in skill is minimal, the decrease in PRESS argues for the incorporation of soil moisture into the model for each station (Table 1.1). Table 1.1 also shows the Durbin-Watson statistic and the heterogeneity of variance test. These statistics are within acceptable ranges. In addition, USGS streamflow station 06625000 has a much higher PRESS value compared to USGS 06620000 for both periods of record. This is attributed to recorded flow at USGS 06620000 being much greater than at USGS 06625000. This is also evident in the standard error of the regression (S).

Extended Record

Identifying Predictors

By extending the period of record, adequate data is available to create the expert system. Of the nine SWE stations within the North Platte River Basin, four were selected based on the "rules" established in the Methods section. One station selected, Deadman Hill, is missing SWE data for 1969. Therefore the value is interpolated using the two closest SWE stations (Roach & Lake Irene). The correlation coefficient between precipitation (October to March) at Steamboat Springs and streamflow (AMJJ volume) for stations 06620000 and 06625000 are 0.75 and 0.76 respectively and they both show stability throughout the extended period of record. This shows that the precipitation records from Steamboat Springs are adequate and will be used in the study. Based on correlation values, and current NRCS methodologies, streamflow persistence is used as a predictor for USGS 06620000, but not as a predictor for USGS 06625000. As mentioned earlier, streamflow data was first recorded in this region in the early 1940's. For USGS streamflow station 06620000, the forecasted period is 1940-2005 (66 years) while 1941-2005 (65 years) is the forecasted period used for USGS station 06625000.

Comparison of Current NRCS Methods with and without ASM

A comparison is made between current NRCS methods and, current NRCS methods incorporating ASM as a predictor for the extended period of record. Table 1.2 shows the numerical measures of skill. By extending the period of record, increased hydrologic variability is incorporated. This variability produces a decrease in overall forecast skill when compared to the limited record. However, by extending the period of record, an expert (decision) system can be developed. For both streamflow stations, there is increase in forecast skill when incorporating soil moisture. For USGS 06620000, an increase from $R^2 = 0.67$ to $R^2 = 0.69$ is achieved after including ASM as a predictor. R^2 values for USGS 06625000 are 0.73 using current forecasting methods and 0.77 after incorporating ASM. The LEPS SK scores for USGS 06620000 are 63.5 without soil moisture and 64.6 incorporating ASM. LEPS SK scores are 66.0 (without ASM) and 66.9 (with ASM) for USGS 06625000. While the authors acknowledge the increases in skill are small, all forecasts produce a higher R^2, predicted R^2, adjusted R^2, and LEPS SK values when incorporating ASM. More importantly, the decrease in PRESS values show that the models incorporating ASM are preferable. Finally, it is important to note that the ASM data used in this research is modeled data that represents an entire climate division (i.e., large spatial area). The author's acknowledge this ASM data is most likely a poor reflection of upper watershed soil moisture, but, this is the best available data (for the extended period of record) in the region. The collection of soil moisture data, from improved land-based equipment or satellites, spatially upstream from the streamflow station(s) will most likely result in even greater improvement in overall model skill. Table 1.2 also shows the Durbin-Watson statistic and the heterogeneity of variance test. The Durbin-Watson statistic for USGS 06625000 (without ASM) is less than the value of dL. This test provides evidence of serial correlation that is accounted for when including ASM.

Expert System Incorporating ASM

ASM is used in an expert system in which three individual forecasts are developed for wet, dry and normal conditions. The number of years for each category are as follows: USGS streamflow station 06620000 (7 dry years, 50 normal years, 9 wet years); USGS streamflow station 06625000 (7 dry years, 49 normal years, 9 wet years). The expert system produces slight to moderate increase in overall skill when compared to the extended period of record forecast (with and without ASM) for both USGS streamflow stations. For example, the expert system results in an R^2 value of 0.73 for USGS 06620000, an increase from 0.67 when forecasting the extended period of record without ASM (i.e., current NRCS methodologies), and an increase from 0.69 when compared to incorporating ASM into the extended period of record. For USGS 0625000, the expert system completes the forecast with an R^2 value of 0.81. This skill is greater than forecasting the extended period of record without soil moisture (R^2 of 0.73) and forecasting the extended period of record with ASM (R^2 of 0.77). As displayed, the expert system results in improved skill when compared to applying NRCS methods (with and without incorporating ASM). Most notably, when current NRCS methods (e.g., without ASM) are compared to expert system results, further (e.g., R^2 increased from 0.67 to 0.73 and 0.73 to 0.81, respectively) improvement in skill is observed. Expert system LEPS SK scores are 64.5 and 70.2 for USGS 06620000 and USGS 06625000, respectively. See Figures 1.2a and 1.2b for a graph showing extended forecasts [without (w/o) ASM and Expert System] plotted versus the streamflow gauge (observed) value.

Improving Poor Forecasts

As previously mentioned, the NRCS has sought improvement in the modeling strategy that will increase the overall skill of the model while specifically providing better prediction of poor forecasts, or those years in which the model provided extremely poor prediction. Poor forecasting is defined in the Methods section. Slight to moderate increase in the measures of overall skill have been previously demonstrated. A “poor” forecast is determined by ranking (worst to best) each year and selecting the upper quartile (25%) of worst forecasts and defining them as “poor” forecasts. These poor forecasts are examined for both the limited and extended periods of record for both stations. Incorporating ASM resulted in a more accurate forecast for six out of the eight worst years for USGS 06620000 (Figure 1.3a), and four out of the six years for USGS 06625000 (Figure 1.3b) when forecasting the limited period of record. An average increase in forecast accuracy of 16% is achieved over these six years for USGS 06620000 when incorporating ASM. Over the 4 years in which including ASM into the model resulted in a better forecast for USGS 06625000, the average increase in forecast accuracy is 10%. For the extended record, incorporating ASM using the expert system approach resulted in a more accurate forecast for 14 out of the 16 poorest forecasted years for both USGS streamflow stations (Figures 1.4a and 1.4b) when compared to the forecast that did not include ASM as a predictor. An average increase in forecast accuracy of 23% is achieved for these 14 years when incorporating ASM for USGS 06620000, and 28% for USGS 06625000. Only six out of the 16 “poor” forecast years are considered extreme (wet or dry) for USGS 06620000 and only five of 16 are extreme based on ASM conditions for USGS 06625000. Therefore, since the majority of NRCS poor forecast years are considered to be normal based on the expert system approach, the process of removing extreme years (both dry and wet) results in improving “normal year” forecast accuracy.

CONCLUSIONS AND FUTURE WORK

The incorporation of ASM into NRCS streamflow forecasting models in the North Platte River Basin achieved both goals set forth by the NRCS. First, overall model skill is improved.

While the author's acknowledge the increase in overall model skill is slight, nevertheless, the decreased value of the PRESS statistic (in all cases) shows statistically that the model that incorporates ASM is the preferred model for forecasting. Second, a notable improvement is observed when attempting to improve "poor" forecasts. The limited period of record resulted in 10 out of 14 "poor" forecasts being improved while the extended period of record resulted in 28 out of 32 "poor" forecasts being improved. The development of an expert (decision) system, based on ASM, is a novel approach that reveals the importance of ASM in streamflow forecasting. While this research provides a basis to consider ASM in streamflow forecasting, there is a considerable void in soil moisture data availability, both in the length of record and the accuracy/precision of the data. Enhanced SNOTEL stations in the North Platte River Basin, that measure soil moisture digitally and in real-time, may result in further increased forecast skill when incorporated as predictors. Inexpensive instrumentation such as conductivity devices and tensiometers can also provide soil moisture data. For both calibrated conductivity-based devices and well-maintained tensiometers, the user can expect measurement accuracies of up to 90 to 95 percent (Murphy 1996). Further research may also incorporate NASA MODIS snow cover data in addition to SNOTEL data. MODIS data will reflect a spatial coverage of snowpack in the basin versus current (SNOTEL) point data. However, one limitation of using MODIS technology includes limited availability of data and digital images. With the increased importance of producing accurate streamflow forecasts, more soil moisture models (and arguably more accurate) are being created. Incorporating this soil moisture data from various available models and instrumentation may prove to be an important predictor in future streamflow forecasts.

REFERENCES

Anderson, T.W. (2003). *An introduction to multivariate statistical analysis* (3rd ed.), John Wiley & Sons, Hoboken, NJ, 461-462.

Aubert, D., Loumagne, C., and Oudin, L. (2003). "Sequential assimilation of soil moisture and streamflow data in a conceptual rainfall-runoff model." *Journal of Hydrology*, 280(1-4), 145-161.

Biondi, F. and Waikul, K. (2004). "DENDROCLIM2002: A C++ program for statistical calibration of climate signals in tree-ring chronologies." *Computers and Geosciences*, 30(3), 303-311.

Day, N. G. (1985). "Extended streamflow forecasting using NWSRFS." *Journal of Water Resources Planning and Management*, 111(2), 157-170.

Garen, D. C. (1992). "Improved techniques in regression-based streamflow volume forecasting." *Journal of Water Resources Planning and Management*, 118(6) 654-670.

Hartmann, H. C., Pagano, T.C., Sorooshian, S. and Bales, R. (2002). "Confidence builders: evaluating seasonal climate forecasts from user perspectives." *Bulletin of the American Meteorological Society*, 83(5), 683–698.

Huang, J., van den Dool, H., and Georgakakos, K.P. (1996). "Analysis of model-calculated soil moisture over the United States (1931-93) and application to long-range temperature forecasts." *Journal of Climate*, 9(6), 1350-1362.

Khattree, R. and Naik, S. (2000). *Multivariate data reduction and discrimination with SAS software*. Cary, NC: SAS Institute Inc., 60-61.

Koch, R. W. (1990). "Influences of climate variability on streamflow variability: implications in streamflow prediction and forecasting." *Final Report for Grant Award*. 14-08-0001-G1316, U.S. Geological Survey, Washington, D.C.

Minitab Inc. (2007). User's Guide. User's Guides.

Montgomery, D.C., Peck, E.A., Vining, G.G. and Myers, R.H. (2006). *Introduction to linear regression analysis* (4th ed.), John Wiley and Sons, Hoboken, NJ, 141-142.

Murphy, A. Tom (1996). "Sensing the elements: moisture sensors and weather stations." *The Irrigation Journal*. <http://www.sowacs.com/sensors/sensingaug.html>.

Myers, R.H. (1990). *Classical and modern regression with applications* (2nd ed.), Duxbury Press, Belmont, CA, 171.

Natural Resources Conservation Service. (n.d.). "Water supply forecasting -- a short primer." Retrieved January 15, 2008, from Natural Resources Conservation Service National Water and Climate Center: <http://www.wcc.nrcs.usda.gov/factpub/wsf_primer.html.>

Pagano, T. C., and Garen, D.C. (2006). "Climate variations, climate change, and water resources engineering."*Integration of climate information and forecasts into western US water supply forecasts*, ASCE Publications, Reston, VA., 86-102.

Pagano, T. C., Erxleben, J. and Perkins, T. (2005). "Operational simulation modeling at the NRCS National Water and Climate Center." *Proc.,Western Snow Conference*, Great Falls, MT., 87-100.

Pagano, T. C., Pasteris, P., Dettinger, M., Cayan, D., and Redmond, K.T. (2004). "Water year 2004: western water managers feel the heat." *EOS T. Am. Geophys. Un*. 85(40), 385-400.

Piechota, T. C., Chiew, F. H. S., Dracup, J. A., and McMahon, T. A. (1998). "Seasonal streamflow forecasting in eastern Australia and the El Niño–Southern Oscillation." *Water Resour. Res.*, 34(11), 3035–3044.

Piechota, T. C., and Dracup, J. A. (1999). "Long range streamflow forecasting using El Niño–Southern Oscillation indicators." *Journal of Hydrologic Engineering*, 4(2), 144–151.

Potts, J. M., Folland, C. K., Jolliffe, I. T., and Sexton, D. (1996). "Revised 'LEPS' scores for assessing climate model simulations and long-range forecasts." *Journal of Climate*, 9, 34–53.

Stedinger, J. R., Grygier, J., and Yin, H. (1988). "Seasonal streamflow forecasts based upon regression." Computerized Decision support systems for water managers; Proc. 3rd Water Resources. *Operations and Mgmt. Workshop*, ASCE, New York, N.Y., 266-279.

Tootle, G. A., and Piechota, T. C. (2004). "Suwannee River long range streamflow forecasts based on seasonal climate predictors." *J. Am. Water Resour. Assoc.*, 40(2), 523–532.

Tootle, G.A., Singh, A.K. Piechota, T.C. and Farnham, I. (2007). Long Lead-Time Forecasting of U.S. Streamflow Using Partial Least Squares Regression. *American Society of Civil Engineers Journal of Hydrologic Engineering*, 12(5), 442-451.

Van den Dool, H., Huang, J., and Fan, Y. (2003). "Performance and analysis of the constructed analogue method applied to U.S. soil moisture over 1981-2001." *Journal of Geophysical Research*, 108(D16), 8617.

Wallis, J. R., D. P. Lettenmaier, and E. F. Wood (1991). "A daily hydroclimatical data set for the continental United States." *Water Resour. Res.*, 27(7), 1657-1663.

Ward, N. M., and Folland, K. K. (1991). "Prediction of seasonal rainfall in the North Nordeste of Brazil using eigenvectors of sea-surface temperature." *Int. J. Climatology*, 11, 711–743.

White, H. (1980). "A heteroskedasticity-consistent covariance matrix estimator and a direst test for heteroskedasticity," *Econometrica*, 48(4), 817-838.

TABLE AND FIGURE CAPTIONS

Table 1.1: Statistics for the limited period of record.

Table 1.2: Statistics for the extended period of record.

Figure 1.1: Location map of Wyoming North Platte River Basin showing used predictors.

Figure 1.2: (a) Extended period of record forecasts (Q gage vs. Q w/o ASM vs. Q Expert) for USGS 06620000.
(b) Extended period of record forecasts (Q gage vs. Q w/o ASM vs. Q Expert) for USGS 06625000.

Figure 1.3: (a) Plot comparing forecasts for the worst quartile of "poor" forecasts using current forecasting methods (NRCS) with proposed methods (incorporating ASM) for USGS 06620000 limited period of record.
(b) Plot comparing forecasts for the worst quartile of "poor" forecasts using current forecasting methods (NRCS) with proposed methods (incorporating ASM) for USGS 06625000 limited period of record.

Figure 1.4: (a) Plot comparing forecasts for the worst quartile of "poor" forecasts using current forecasting methods (NRCS) with proposed methods (expert system) for USGS 06620000 extended period of record.
(b) Plot comparing forecasts for the worst quartile of "poor" forecasts using current forecasting methods (NRCS) with proposed methods (expert system) for USGS 06625000 extended period of record.

Table 1.1

	USGS 06620000 w/o ASM	USGS 06620000 w/ASM	USGS 06625000 w/o ASM	USGS 06625000 w/ASM
Period of Record	1979-2005 (27)	1979-2005 (27)	1983-2005 (23)	1983-2005 (23)
R^2	0.82	0.83	0.79	0.82
R^2(adj)	0.81	0.82	0.78	0.81
R^2(pred)	0.79	0.81	0.76	0.80
PRESS	90,535.17	87,107.75	17,429.70	14,800.00
S	56.80	55.30	26.81	24.83
Durbin-Watson	2.12	2.42	1.63	1.97
dL	1.24	1.24	1.26	1.26
dU	1.56	1.56	1.44	1.44
S""	18.96	19.2	15.04	15.54
SK	70.24	71.03	65.40	67.57
c_0	4.58	4.18	1.46	1.69
p_c	0.47	0.52	0.48	0.43

Table 1.2

	USGS 06620000 w/o ASM	USGS 06620000 w/ASM	USGS 06625000 w/o ASM	USGS 06625000 w/ASM
Period of Record	1940-2005 (66)	1940-2005 (66)	1941-2005 (65)	1941-2005 (65)
R^2	0.67	0.69	0.73	0.77
R^2(adj)	0.67	0.69	0.72	0.76
R^2(pred)	0.65	0.67	0.70	0.74
PRESS	286,191.85	269,145.60	48,715.10	42,312.50
S	65.00	63.00	26.50	24.60
Durbin-Watson	1.90	2.07	1.28	1.73
dL	1.57	1.57	1.53	1.50
dU	1.63	1.63	1.66	1.70
S""	18.96	19.18	42.83	43.47
SK	70.24	71.03	65.90	66.88
c_0	0.56	0.67	8.93	11.51
p_c	0.76	0.72	0.11	0.24

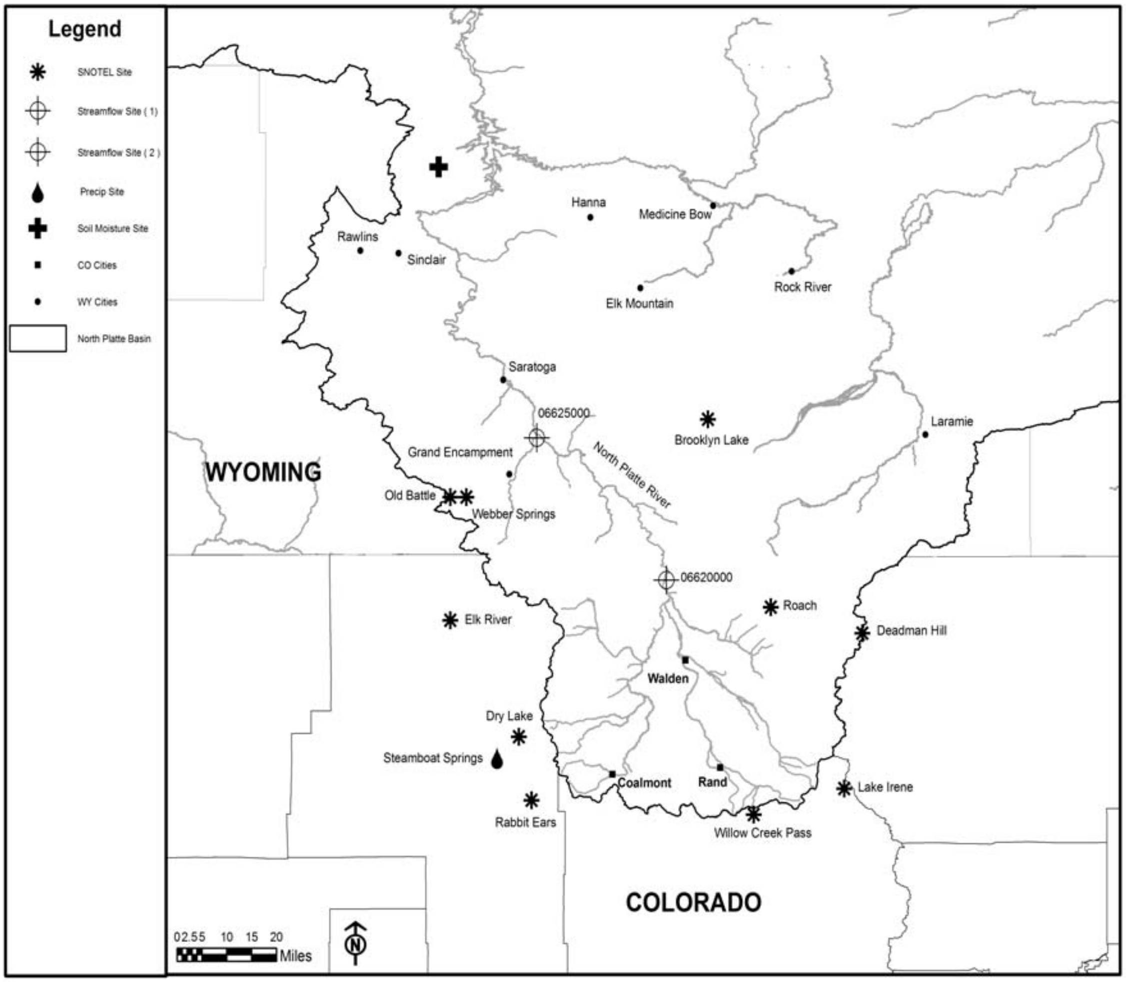
Legend
SNOTEL Site
Streamflow Site (1)
Streamflow Site (2)
Precip Site
Soil Moisture Site
CO Cities
WY Cities
North Platte Basin
Hanna
Medicine Bow
Rawlins
Sinclair
Elk Mountain
Rock River
Saratoga
06625000
Brooklyn Lake
Laramie
Grand Encampment
North Platte River
WYOMING
Old Battle
Webber Springs
06620000
Roach
Elk River
Deadman Hill
Walden
Dry Lake
Steamboat Springs
Coalmont
Rand
Lake Irene
Rabbit Ears
Willow Creek Pass
COLORADO
02.55 10 15 20
Miles
N

Figure 1.1

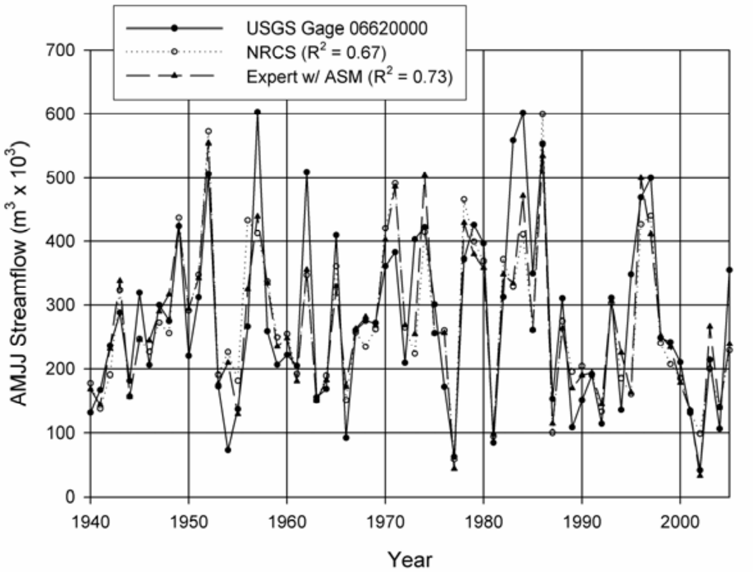

Figure 1.2(a)

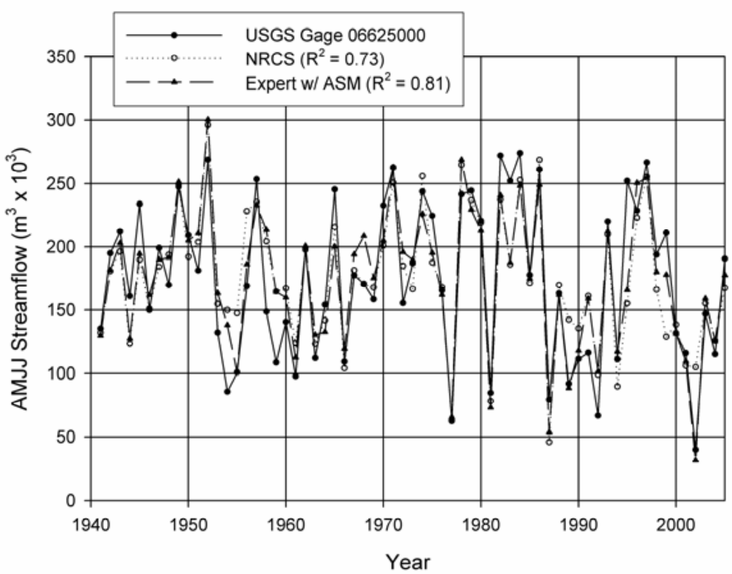

Figure 1.2(b)

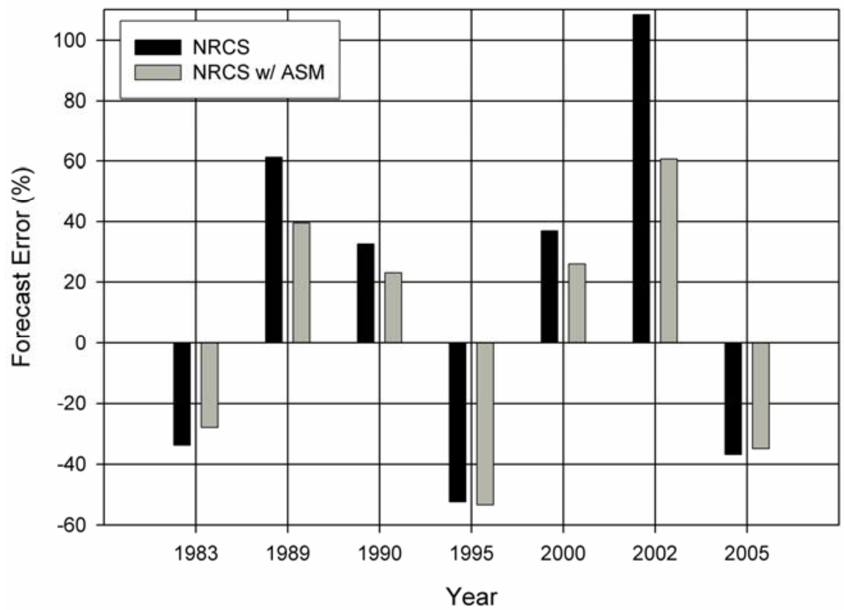

Figure 1.3(a)

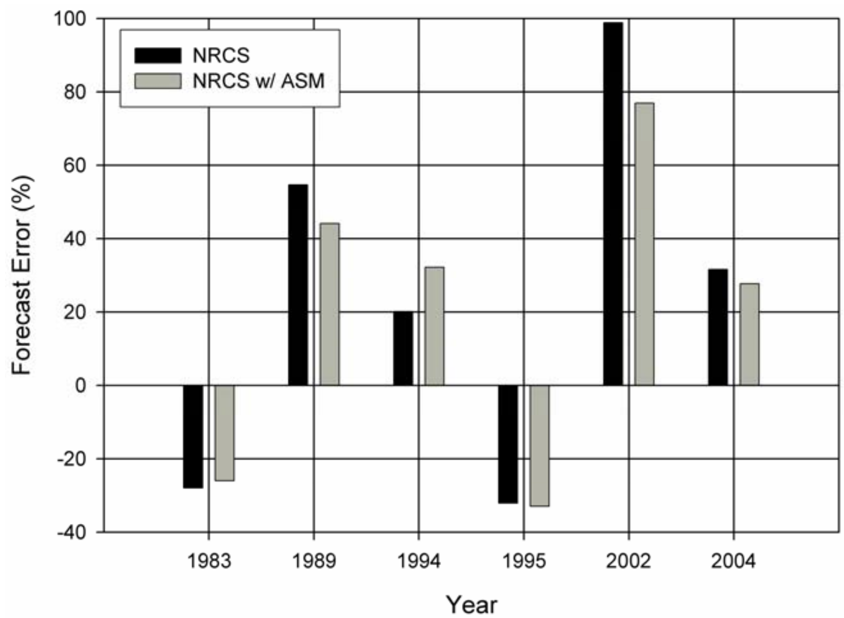

Figure 1.3(b)

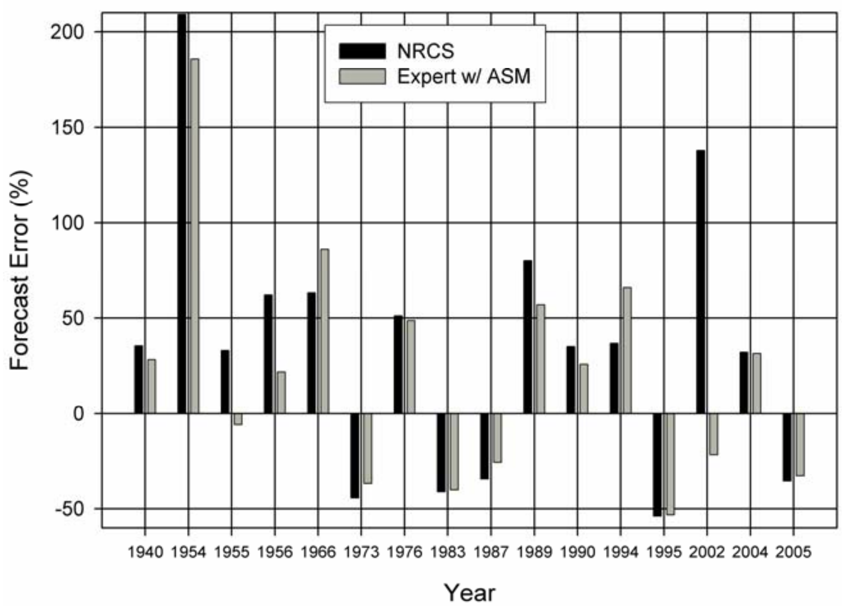

Figure 1.4(a)

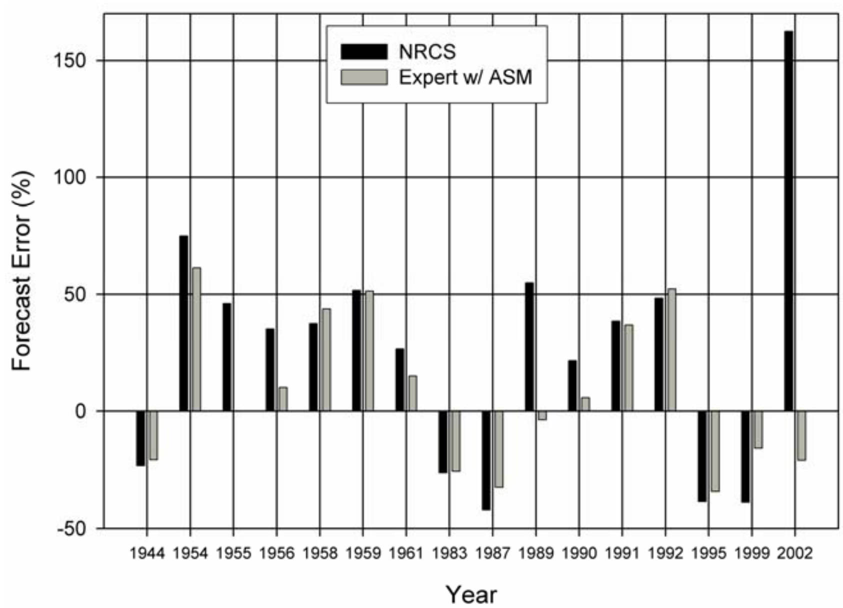

Figure 1.4(b)

CHAPTER 2 - Long Lead-time Streamflow Forecasting of the North Platte River Incorporating Oceanic-Atmospheric Climate Variability

ABSTRACT

An evaluation of the influence of oceanic-atmospheric climate variability on streamflow in the upper North Platte River basin is presented. Through the application of Singular Value Decomposition (SVD) statistical methods, sea surface temperatures (SSTs), 500 mbar geopotential height (Z_{500}) values and North Platte streamflow were evaluated over a historical period from 1948 to 2006. This resulted in the identification of new regions of highly correlated SSTs and Z_{500} that may not be represented by existing index regions (Niño 3.4 —defined El Nino Southern Oscillation region, PDO--Pacific Decadal Oscillation, and AMO—Atlantic Multidecadal Oscillation). A long lead-time approach was utilized such that a three month lead-time (seasonal average of monthly SSTs or Z_{500} for October, November and December) as well as a six month lead-time (seasonal average of monthly SSTs or Z_{500} for July, August and September) of previous year variability were used as predictors for the following year spring streamflow (seasonal monthly average of April, May, June and July). Temporal expansion series from SVD were utilized as predictors in a non-parametric model to develop continuous exceedance probability forecasts. The results displayed good skill using SSTs for the six month lead-time forecast and excellent skill using Z_{500} values for the three month lead-time forecast. The improved skill found over basic climatology forecasts will be useful to water managers when trying to predict and manage expected streamflow volumes several months in advance.

INTRODUCTION

Over the past several decades, hydrologists and climatologists have developed relationships between large scale oceanic-atmospheric variability and climate (hydroclimatology). Atmospheric – oceanic climatic and sea surface temperature (SST) variability can provide important predictive information about hydrologic variability in regions around the world. Significant research has focused on identifying atmospheric – oceanic climatic phenomena such as the El Niño-Southern Oscillation (ENSO) [Philander, 1990], the Pacific Decadal Oscillation (PDO) [Mantua, et al., 1997] and the Atlantic Multidecadal Oscillation (AMO) [Enfield et al., 2001]. Further research has identified what influence these phenomena have on U.S. hydrology, including streamflow and snowpack [e.g., Cayan and Peterson, 1989; Cayan and Webb, 1992; Kahya and Dracup, 1993, 1994a and 1994b; Enfield et al., 2001; Rogers and Coleman, 2003; Maurer et al., 2004; McCabe et al., 2004; Tootle et al, 2005, Hunter et al., 2006]. The relationships between atmospheric – oceanic climate variability may result in their utilization as long lead-time (e.g., three to six months) predictors (forecasters) of various hydrologic responses, including streamflow.

Streamflow forecasting is the process of predicting the volume of water at a specific location for a specific time period. Currently, the Natural Resources Conservation Service (NRCS) and the National Weather Service (NWS) cooperate to generate forecasts around the first of each month between January and June. Nearly all of these forecasts are produced using parametric statistical approaches such as multiple linear regression models [NRCS, 2007]. An alternative to typical parametric regression techniques is a non-parametric approach

Non-parametric routines avoid the usual assumption that the data comes from a normal distribution (or any specific distribution). Essentially, a non-parametric model is derived from the data and does not pre-define the form (i.e. linear or non-linear) of the function. Non-parametric methods have been successfully applied to streamflow forecasting. Lall [1995] performed an extensive analysis of applications of non-parametric probability uses in stochastic hydrology. Several other non-parametric methods (K nearest neighbor local polynomials and local weighted polynomials) have been successfully applied to hydrologic (and streamflow) forecasting [Lall and Sharma, 1996, Rajagopalan and Lall, 1999, Souza and Lall, 2003]. Piechota and Dracup [1999] applied non-parametric (kernel density estimator) methods to forecasting streamflow for long lead-times and showed significant improvement when comparing the results to the climatology (no skill) forecast [Piechota and Dracup, 1999]. The non-parametric kernel density estimator was also successfully applied to El Niño-Southern Oscillation (ENSO) affected streams in eastern Australia and Florida [Piechota et al., 1998, Tootle and Piechota, 2004]. The exceedance probability forecast developed provides an example of applying non-parametric techniques to forecasting. An exceedance probability forecast explains the likelihood that a certain streamflow volume will be equaled or exceeded during a certain period of time. Exceedance probability forecasts are used for the design and operation of water resource systems that require a high degree of system reliability [Piechota et al., 2001]. However, whether applying parametric or non-parametric techniques (utilizing climate variability), it is vital to identify statistically strong relationships (predictors) between climate variability and streamflow response.

Several methods are typically used to determine the relationship between two spatial-temporal arrays of data such as climate variability (e.g., SSTs) and streamflow. Common methods include correlation analysis, principal component analysis and singular value decomposition (SVD). Bretherton et al. [1992] evaluated several statistical methods and concluded SVD was simple to perform and preferable for general use. In a study between wintertime sea surface temperature and 500 mbar height (Z_{500}) anomalies, Wallace et al. [1992] determined that SVD isolates the most important modes of variability as well as discovering a coupling between the interannual variability of SST and Z_{500} due to their common link with global wave patterns. SVD has been used to identify relationships between oceanic SST variability and hydrologic variability. Wang and Ting [2000] evaluated Pacific Ocean SSTs and continental U.S. precipitation for concurrent (overlapping) time periods and identified simultaneous patterns of SST influence on precipitation. Uvo et al. [1998] applied SVD to evaluate Pacific and Atlantic Ocean SSTs (independently) and northeast Brazilian precipitation utilizing both a simultaneous and lagged approach. Rajagopalan et al. [2000] utilized SVD and applied a lag approach to evaluate global SST impacts on continental U.S. drought. Shabbar and Skinner [2004] applied SVD and utilized a lag approach in which winter global SSTs and summer Canadian drought [e.g., Palmer Drought Severity Index (PDSI) values] were evaluated and determined each mode representing a distinct oceanic / atmospheric phenomena (e.g., 1st mode – AMO, 2nd mode – ENSO, 3rd mode – PDO). Tootle and Piechota [2006] analyzed Pacific and Atlantic Ocean SSTs which resulted in the identification of several SST regions associated with streamflow regions in the continental United States. Tootle et al. [2008] applied this approach (SVD) to Pacific and Atlantic SSTs and Colombia streamflow, identifying several SST and streamflow regions of significance.

When examining the impacts of oceanic-atmospheric climate variability, a significant influence on that variability comes from various dynamics at different pressure levels in the atmosphere. In order to reference the height of the various pressure regimes, the term geopotential height is used. In essence, geopotential height is the height to the pressure zone of interest, as measured above the mean sea surface elevation. Blackmon [1976] did a study of the 500 mbar geopotential height (Z_{500}) of the northern hemisphere which presented long term averages of atmospheric parameters. Through a comparison, described in the study, interannual variability can be obtained and would allow for a comparison of various data sets and thus generate a circulation model that has the ability to replicate the atmosphere's behavior in low to mid frequency domains and in various spatial scales. Building upon the 1976 study, Blackmon [1977] explored the behavior of the 500 mbar wind statistics upon northern hemisphere wintertime circulation. The results of these studies suggested that Z_{500} index values can be attributed to substantial impacts on climate. On a global level Xoplaki et al. [2000] determined that the link between precipitation over Greece and changes in large scale atmospheric circulation are strong, specifically in relation to 500 mbar geopotential heights. As related to the work of this paper, Serreze et al. [1998] evaluated the relationship between snowfall and low frequency atmospheric variability and found that the troughs and ridges associated with the 500 mbar zone do play a role in the characteristics of snowfall over the eastern United States. Grantz et al. [2005] explored the impacts of including Z_{500} height index values as predictors in streamflow forecasting models and discovered an improved skill with such an addition.

The North Platte River (Figure 2.1) originates in north central Colorado with tributaries and contributing basins predominately located in mountainous regions of Colorado and Wyoming. As a result, most of the annual streamflow can be attributed to melting snowpack that has accumulated during the winter and early spring months in the mountainous headwater regions. The North Platte River flows north into Wyoming, then east to Nebraska. Present and future use of water resources in the North Platte River Basin (NPRB) are heavily regulated and controlled by the Supreme Court Decree for the North Platte River [North Platte River Basin Overview, 2008]. Recent lawsuits regarding interstate water allocations have augmented the need for a more skillful and longer lead-time forecast. Currently, only parametric (regression) models are used to develop a relationship between predictor variables (precipitation, snow water equivalent, antecedent streamflow, etc.) and the predictand (April-May-June-July streamflow volume). From a forecasting perspective, the challenge with the NPRB is the lack of a distinct climate signal (e.g. ENSO, PDO, AMO) per research performed on unimpaired streamflow and snowpack in the continental and western U.S. [Tootle et al., 2005; Hunter et al., 2006]

The proposed research will develop a unique long lead-time (three to six months) streamflow forecast of unimpaired streamflow stations in the NPRB utilizing oceanic-atmospheric climate information. Similar to Grantz et al. [2005], Pacific and Atlantic Ocean SST variability and Z_{500} index values will be utilized as predictors. However, in lieu of using correlation to identify predictors, SVD techniques will be applied to identify spatial regions of SSTs and Z_{500} that relate to streamflow variability in the NPRB. Additionally, a non-parametric approach will be utilized to develop an exceedance probability streamflow forecast comparable to the work of Piechota et al. [2001].

DATA

Streamflow Data

Data from four unimpaired streamflow stations (Q1 - #06620000, Q2 - #06625000, Q3 - #06630000 and Q4 - #06635000) in the Upper North Platte River Basin (Figure 2.1) were obtained from the U.S. Geological Survey (USGS) National Water Information System [USGS, 2008]. USGS provides historical monthly mean streamflow in cubic feet per second (cfs). The average monthly streamflow rate in cfs for April, May, June and July (AMJJ) were summed and converted into streamflow volumes using appropriate conversions. The period of streamflow volume used in the analysis was 1949 to 2006 (57 years).

Climatic Indices

Three of the applicable predefined datasets representing oceanic – atmospheric climatic phenomena are the Niño 3.4 index, the PDO index and the AMO index. The average monthly values for the climatic indices (Niño 3.4, PDO and AMO) were averaged for the six month lead-time period of July, August and September [JAS(-1)] as well as for the three month lead-time period of October, November and December [OND(-1)]. The (-1) nomenclature identifies that the predictor periods are for the previous year to the predictand, AMJJ streamflow. The time span averaged was 1948 to 2005 (57 years) and preceded the streamflow volumes used by one year.

The Niño 3.4 [Trenberth, 1997] SST region is located along the equatorial Pacific Ocean (5P^{oP}S – 5P^{oP}N, 170P^{oP} – 120P^{oP}W) and monthly index data were obtained from the NOAA ESRL Physical Sciences Division [http://www.cdc.noaa.gov/Pressure/Timeseries/Nino34/]. The Niño 3.4 index was used since it is an overall representation of ENSO. The PDO is a oceanic / atmospheric phenomena associated with persistent, bimodal climate patterns in the northern Pacific Ocean (poleward of 20P^{oP} north) that oscillate with a characteristic period on the order of 50 years (a particular phase of the PDO will typically persist for about 25 years) [Mantua, et al., 1997; Mantua and Hare, 2002]. PDO Index [Mantua et al., 1997, Hare and Mantua, 2000] values were obtained from the Joint Institute for the Study of the Atmosphere and Ocean, University of Washington [http://tao.atmos.washington. edu/pdo/]. The Atlantic Multidecadal Oscillation (AMO) index was introduced by Enfield et al. [2001] as a simple basin average of North Atlantic Ocean (0 to 70P^{oP}) sea surface temperatures (SSTs). The AMO index consists of detrended (dividing, centering and re-scaling the data to account for unimodal data sets) SST anomalies for the previously defined Atlantic Ocean region. AMO index values are available from the National Oceanic and Atmospheric Administration (NOAA) ESRL Physical Sciences Division [http://www.cdc.noaa.gov/Pressure/Timeseries/].

Pacific and Atlantic Ocean Sea Surface Temperature Data

SST data for the Pacific and Atlantic Oceans were obtained from the National Climatic Data Center [http://www.cdc.noaa.gov/cdc/data.noaa.ersst.html]. The oceanic SST data consists of average monthly values for a 2^o by 2^o grid cell [Smith and Reynolds, 2004]. The extended reconstructed global SSTs were based on the Comprehensive Ocean-Atmosphere Data Set (COADS) from 1854 to present [Smith and Reynolds, 2003].

The overall gridded data region of Pacific Ocean SST data used for the analysis was longitude 100°E to longitude 80°W and latitude 30°S to latitude 60°N while the region of Atlantic Ocean SST data used for the analysis was longitude 80°W to longitude 20°W and latitude 30°S to latitude 60°N. The longitudinal boundaries of this study (100°E to 20°W) extended the regions of Grantz et al. [2005] (100°E to 60°W) to encompass the possibility of more Atlantic ocean influences while the latitudinal boundaries were identical. Similar regions were explored by Tootle and Piechota [2006] due to these regions representing the majority of oceanic—atmospheric climate influences on U.S. climate (i.e., storm tracks such as Pacific Ocean frontal storms). The regions selected were also similar to other studies, such as those of Wang and Ting [2000]. Similar to the climate indices, average monthly values were averaged for the predictor seasons [JAS(-1) and OND(-1)] for each SST cell.

500 mbar Geopotential Height Index Data (Z_{500})

The monthly Z_{500} index data are a product of the NCEP/NCAR Reanalysis 40-year Project [Kalnay et al., 1996] and can be obtained from the NOAA Physical Sciences Center [http://www.cdc.noaa.gov/cgi-bin/Composites/printpage.pl]. The Z_{500} index data are given on a 2.5° x 2.5° latitude and longitude grid and are available from 1948 to 2008. The overall gridded data region of data used for the analysis was longitude 100°E to longitude 20°W and latitude 30°S to latitude 60°N, similar to the previously described SST regions. Like the SSTs, average monthly values were averaged for the predictor seasons [JAS(-1) and OND(-1)] for each Z_{500} cell.

METHODS

Climate/Streamflow Relationships

Comparable to Grantz et al. [2005], the first step was to analyze relationships between potential predictors and predictands. The relationship between ocean-atmospheric variability and streamflow was examined through the development of a correlation table. The correlation table was created using typical correlation techniques between the seasonal [JAS(-1) and OND(-1)] climate indices (Niño 3.4, PDO and AMO) and the four streamflow (AMJJ) stations (Q1, Q2, Q3, Q4).

Singular Value Decomposition (SVD)

Grantz et al. [2005] examined the relationships between streamflow and oceanic-atmospheric signals using visual inspection of correlation maps and composite analyses. The work presented here builds upon that methodology through the use of SVD. SVD is a powerful statistical tool for identifying coupled relationships between two, spatial-temporal fields. Bretherton et al. [1992] provides a detailed discussion of the theory of SVD, while Tootle et al. [2008] and Tootle and Piechota [2006] provide a brief description of SVD, as applied in the current research.

Initially, a matrix of standardized SST (or Z_{500}) anomalies and a matrix of standardized streamflow anomalies (for the four NPRB stations) were developed. The time dimension of each matrix (i.e., 57 years) must be equal while the spatial component (i.e., SST cells or Z_{500} and North Platte streamflow stations) can vary in dimension. The cross-covariance matrix was then computed for the two spatial, temporal matrices and SVD was applied to the cross-covariance matrix and physical information regarding the relationship between the two was obtained. The resulting SVD of the cross-covariance matrix created two matrices of singular vectors and one matrix of singular values. The singular values were ordered such that the first singular value (1^{st} mode) was greater than the second singular value and so on. Bretherton et al. [1992] defines the squared covariance fraction (SCF) as a useful measurement for comparing the relative importance of modes in the decomposition. Each singular value was squared and divided by the sum of all the squared singular values to produce a fraction (or percentage) of squared covariance for each mode.

Finally, the two matrices of singular vectors were examined, generally referred to as the left (i.e., SST or Z_{500}) matrix and the right (i.e., streamflow) matrix. The first column of the left matrix (1^{st} mode) was projected onto the standardized SST or Z_{500} anomalies matrix and the first column of the right matrix (1^{st} mode) was projected onto the standardized streamflow anomalies matrix. This resulted in the 1^{st} temporal expansion series of the left and right fields, respectively. The left heterogeneous correlation figure (for the 1^{st} mode) was determined by correlating the SST or Z_{500} values of the left matrix with 1^{st} temporal expansion series of the right field and the right heterogeneous correlation figure (for the 1^{st} mode) was determined by correlating the streamflow values of the right matrix with the 1^{st} temporal expansion series of the left field. The left temporal expansion series have a physical meaning since they represent SST or Z_{500} variability that may not already be included in existing SST indices and could represent a new index of SST variability. This may then be useful in forecasting streamflow for stations that have high correlations with the temporal expansion series. Utilizing an approach similar to Rajagopalan et al. [2000] and Uvo et al. [1998], heterogeneous correlation figures displaying 90% significant correlation values for SST and Z_{500} regions were reported. These reported correlations statistically differ from zero at a 10% significance level. A 10% significance level was selected to balance the need to identify correlations that differ from zero, while also recognizing that the relationships between SSTs and Z_{500} is subtle. As a result, correlations which are large in magnitude may not be detected at smaller significance level (e.g., 1%). While SVD is a powerful tool for the statistical analysis of two spatial, temporal fields, there exist several limitations to its use that should be investigated [Newman and Sardeshmukh, 1995]. Generally, if the leading (1^{st}, 2^{nd}, 3^{rd}) modes explain a significant amount of the variance of the two fields, then SVD can be applied to determine the strength of the coupled variability present [Newman and Sardeshmukh, 1995]. However, when using SVD to examine two fields, the examiner must exhibit caution when attempting to explain the physical cause of the results [Newman and Sardeshmukh, 1995].

Forecast Methodology

The streamflow forecast developed is a continuous exceedance probability curve that can be used for any assumed risk level and was developed by Piechota et al., [2001]. The "no skill / climatology" forecast curve is generated by dividing the rank of each historical value by the total number of years in the record.

Two advantages are found using the model developed by Piechota et al. [2001]: it considers the continuous relationship between the predictand and the predictor, and it does not assume a particular model structure. It suffers, however, from its semi-empiricism; fitting the model to the data points assumes that the historical data represents the entire population. A detailed description of the methodology and model can be found in Piechota et al., [2001] and Piechota et al., [1998]. A brief description of the model (for one predictor) is provided below:

1. The climate predictor values (Pi) for each year and the corresponding streamflow predictand values (Qi) for each year are compiled, where (Pi) represents the temporal expansion series obtained from SVD, as described in the methods section, for SSTs or Z500 index values.
2. The streamflow values (Qi) are ranked in ascending order and the corresponding climate predictor (Pi) for the corresponding year of the streamflow are noted.
3. The first data point for analysis occurs immediately after the five lowest streamflow values (Qi) and the last point for analysis occurs immediately prior to the five highest streamflow values (Qi). This is required since a minimum of five values are needed to generate a probability density function.
4. The first data point for analysis is the sixth ranked streamflow value (lowest to highest) based on #3 above. Using the kernel density estimator (Silverman, 1986 and Piechota et al., 1998), a probability density function is developed for all climate predictor values below the first data point and a probability function is developed for all climate predictor values above the first data point. Whereas f(x) is the probability density function expressed as,

$$f(x) = \frac{1}{hn}\sum_{i=1}^{n} [k\left(\frac{x - x_i}{h}\right)]$$

$$h_i = .9A_i n_i^{-\left(\frac{1}{5}\right)}$$

$$A_i = \min\left(\sigma_i\ ,\ \frac{interquartile\ range}{1.34}\right)$$

where,

- X_1 to X_i is a set of n observations
- k( ) is the kernel function
- h is the bandwith
- optimal h = h_i
- σ_i is the stdev of predictor data in each subset i
- n_i is the # of observations in each subset.

and the Bayes probability theorem is expressed as,

$$Prob\left(\frac{Q_i}{x}\right) = \frac{P_i f_i(x)}{\sum_{i=1}^{k} P_i f_i(x)}$$

where,

- X = predictor value
- Q_i = streamflow
- P_i = prior probability streamflow
- f_i (x) = probability density function of prior X value

5. A unique probability value is determined for each predictor value, given the sixth ranked streamflow value. These values are single points on the exceedance probability curve (Probability versus Streamflow). The procedure is then repeated for the seventh ranked streamflow value and so on.
6. An exceedance probability is then determined for each predictor value. The forecast curve will represent the probability of exceeding a value of streamflow, based on the value of the predictor.
7. The final exceedance probability forecast is found by combining the three individual forecasts into one combination forecast that has better overall skill. The combination forecast is found by applying weights a, b, and, c to the three models so that the weights add up to one. The optimal forecast is found by applying more weight to individual forecasts that better predicts streamflow and less weight to poor individual forecasts. These optimal weights are determined by an optimization procedure that evaluates the Linear Error in Probability Space (LEPS) score for all possible combinations, using weighting increments of 0.02 in which the weights vary between 0 and 1 for each model. The final combination forecast is the model with the highest LEPS score.

The skill of the forecast, as produced by the model, was measured using the Linear Error in Probability Space (LEPS) score. The LEPS score is a measure of skill that was originally developed to assess the position of the forecast and the position of the observed values in the cumulative probability distribution (non-exceedance probability); the LEPS score can be used for continuous and categorical variables [Ward and Folland, 1991; Potts et al., 1996]. A modified LEPS score is required due to the absence of a convenient measure of skill for an exceedance probability forecast. A better measure of skill is one in which more weight is given to a forecast that effectively predicts low or high flow and less weight to a forecast that successfully predicts average flow. The application of the LEPS score is desirable here because it is less sensitive to changes near the center of the cumulative probability distribution and more sensitive to forecasts of high or low values. Essentially, it rewards a successful forecast of extreme values [Piechota et al., 2001]. The developmental steps and the equations used to generate a LEPS score for an exceedance probability forecast can be reviewed in Piechota et al. [2001] and a brief description is hereby provided. In terms of probability, the LEPS score measures the distance between the forecast and observed values. First, a “no skill” or “climatology” curve was developed for the observed yearly streamflow values. The “climatology” curve was created by ranking observed yearly streamflow values in decreasing order (i.e., exceedance probability) of magnitude and dividing the rank of each observed value by the total number of years in the record. The LEPS score is defined as

$$S'' = 3 * (1 - |Pf - Po| + Pf2 - Pf + Po2 - Po) - 1$$

where Pf and Po are the forecasted and observed cumulative probabilities, respectively. The LEPS score was calculated for each year and “good” or “bad” forecast years were identified. The average skill (SK) is defined as

$$SK = \frac{\sum 100 S''}{\sum S''_m}$$

where the summation S” is for all years of record. If S” is positive, S”m is the sum of the best possible forecast (i.e. Pf = Po) for all years of record. If S” is negative, S”m is the sum of the worst possible forecast (i.e. Pf = 1 or 0) for all years of record. A LEPS SK score of greater than +10% is generally considered good skill.

The skill associated with each individual forecast is calculated for calibration and cross-validation analyses. The LEPS score for the calibration analysis does not provide an independent skill score because it is based on the same data in which the model was calibrated. To report the skill scores explained in the results section, each individual yearly calibrated and cross validated LEPS skill score was averaged over the entire 57 year period of record to develop an overall average forecast skill. Additionally, various combinations of different predictors (i.e. AMO, SST1, 500 mb1, Niño 3.4, SST1, 500mb1) were modeled in an attempt to obtain an optimal weight amongst the various predictors.

RESULTS

Climate Indices

As shown in Table 2.1, and as similarly reported by Grantz et al. [2005], the standard indices did not show significant relationships with spring streamflow volumes at any of the locations. Consequently, as described by Grantz et al. [2005], an investigation between large-scale oceanic-atmospheric variability and its link with streamflow was examined as a potential predictor.

When correlating the PDO index with the four previously defined streamflow stations (AMJJ volume) for both three and six month [JAS(-1)] lead-times, the correlation values resulted in no stations exceeding 90% significance. Similarly, the Niño 3.4 index resulted in none of the four stations exceeding 90% significance for either time period. The Niño 3.4 and PDO correlation coefficient values for both JAS(-1) and OND(-1) for Q1, Q2, Q3 and Q4 are close to 0 and therefore conclude that the Niño 3.4 and PDO signals are not prominent in the upper NPRB. When correlating the AMO index, all four stations exceeded 90% significance for the JAS(-1) (six month) lead-time period, whereas only one exceeded 90% significance for the three month lead-time. The AMO displays a stronger presence in the NPRB, as shown by its higher correlation coefficient values; however the coefficient values are not strong enough to form the basis for a skillful forecast. The correlation analysis was a preliminary study which verified the need to generate regions through the use of SVD that showed a significant relationship to the NPRB. Additionally, each predefined climate index was analyzed through the forecast model such that calibration and cross validation skill was reported. As explained by Tootle and Piechota [2004], calibration uses all of the data to calibrate the weights and then computes the skill based on all the data. Table 2.2 shows the weights (in percentage) applied by the cross validation model to each index. The calibration and cross validated skill score, also in percentage, are displayed immediately below the weights values. The weights displayed show that for JAS(-1), 100% of the weight to develop the cross validated exceedance probability forecast was applied to the AMO signal. The LEPS scores for the calibration analysis were greater than +10% for Q2 and Q4. However, cross-validation provides a more independent assessment of the forecast skill and of the weights applied to each model [Elsner and Schmertmann, 1994; Michaelsen, 1987]. Cross-validation allows the model to remove a year, calibrate the model, and then test the model on the year that was removed. This procedure is repeated for all years. The use of cross-validation eliminates spurious predictors and artificial skill. The LEPS score for the cross-validation analyses drops considerably when compared to the LEPS score for the calibration analysis. It can be reasoned that a good forecast would be indicated by a cross-validated LEPS score at or above +10%, which is not evident in any of the climate index results. The highest cross validated skill score for the JAS(-1) was the model run with Q4 and the AMO index, resulting in a value of 1.4%. The results of the OND(-1) run exhibit different behavior in terms of the weights being split amongst different signals. The Q1 run resulted in 33% of the forecast weight being placed on the Niño 3.4 signal. Different weights are selected by the model in an attempt and achieve the most skillful forecast. The weights selected by the model for each run are shown in Table 2.2. The calibration scores are all below +10% as well as all of the cross validated LEPS score values being negative, indicating the climate indices for the OND(-1) are poor predictors of streamflow volume in the NPRB.

Sea Surface Temperatures (SSTs)

When applying SVD to Pacific / Atlantic Ocean SSTs and North Platte streamflow, this resulted in squared covariance fractions (SCF) of 84.3% - 1st mode, 12.7% - 2nd mode and 1.7% - 3rd mode for the JAS(-1) lead-time period. The OND(-1) lead-time period resulted in SCFs of 81.2% - 1st mode, 15.3% - 2nd mode and 2.0% - 3rd mode. Therefore, for both lead-times, the 1st mode clearly identifies the strongest relationships. The total number of Pacific / Atlantic Ocean SST cells was 4329. For the 1st mode of JAS(-1) variability, 528 Pacific / Atlantic Ocean SST Cells (12.2%) were identified as significant. Figure 2.2 represents heterogeneous correlation maps (90% significance or $|r| > 0.21$) displaying significant Pacific / Atlantic Ocean SST for the 1st mode of SVD for the JAS(-1) lead-time. All four North Platte River streamflow stations were identified as being significant. For the 1st mode of OND(-1) variability, 493 Pacific / Atlantic Ocean SST Cells (11.4%) were identified as significant. Modes 2 and 3 were not reported based on the lack of significance of the SCF for both lead-times.

The results of the forecast model runs for JAS(-1) and OND(-1) are presented in Table 2.2. The table displays the temporal expansion series as row headings, for modes 1, 2 and 3 (SST1, SST2, SST3 respectively) of the SVD analysis, on the left. The weights applied to each temporal expansion series are displayed as a percentage, for the respective streamflow station (Q1, Q2, Q3 and Q4). The model applied 100% of the weight of the forecast on the first mode temporal expansion series (SST1). The 100% weighting acknowledges that the region defined through the SVD analysis for mode 1 has the strongest spatial-temporal relationship [84.3% -- JAS(-1) and 81.2% -- OND(-1)] and consequently is the best predictor for all four streamflow stations. The calibration and cross validated LEPS skill scores displayed in Table 2.2 are averages over the entire period of analysis (57 years). The six month lead-time [JAS(-1)] calibration LEPS skill scores are all above +10%. Even more appealing are the results of the JAS(-1) cross validated LEPS skill scores. Three of the four stations exhibit a cross-validated skill score near +10% with Q4 actually surpassing +10% with a value of +10.2%. For the three month lead-time forecast [OND(-1)], the calibrated skill scores were close to those of the six month lead-time scores. However, the cross-validated skill scores show a general decrease in skill value, with the most skillful result being +6.2% for Q2. It should be noted that for both lead-time periods, the cross validated skill for all analyses are above zero, indicating that the forecast model has better skill than the climatology forecast (skill = 0). Figure 2.3 presents examples of poor and good exceedance probability forecasts for individual years for each streamflow station for the JAS(-1) lead-time. For example, the 1963 Q2 vs. JAS SST represents a good forecast (cross validated

LEPS score of 61.17%). Using this graph, a water manager, assuming a 50% risk level (50% exceedance) would have correctly projected an average AMJJ streamflow volume of 1.12 x 10^8 cubic meters (m^3). Utilizing the climatology forecast at a 50% exceedance level, the water manager would have over-forecasted the projected supply at 1.75 x 10^8 m^3 .On the same note, there are risks associated with poor forecasts. Using the 1996 Q1 vs. JAS SST graph as an example of a poor forecast (cross validated LEPS score of -61.08%), a water manager assuming a 50% risk (50% exceedance) would have predicted a streamflow volume of 2.01 x 10^8 m^3 when in fact 4.69 x 10^8 m^3 was actually reported. Nevertheless, by averaging the entire period of record (57 years), for each streamflow station, the positive cross validated skill score is relatively close to +10%. This provides evidence for a greater number of good forecasts than poor forecasts.

500 mbar Geopotential Height Index

SVD analysis of 500 mbar Geopotential Height Index values and North Platte streamflow resulted in squared covariance fractions (SCF) of 70.3% - 1st mode, 24.1% - 2nd mode and 3.4% - 3rd mode for the JAS(-1) lead-time. SCFs for the OND(-1) lead-time were 73.4% - 1st mode, 22.0% - 2nd mode and 2.5% - 3rd mode. The 1st mode of variability (only) was reported, based on the significant squared covariance fraction reported for the 1st mode. The total number of Z_{500} Cells was 3589. For the 1st mode of variability and the JAS period, 94 Z_{500} Cells (2.6%) were identified as significant. For the 1st mode of variability and the OND(-1) period, 207 Z_{500} Cells (5.8%) were identified as significant. OND(-1) heterogeneous correlation maps (90% significance or $|r| > 0.21$) displaying significant Z_{500} regions and North Platte River streamflow stations for the 1PstP mode of SVD are shown in Figure 2.4.

Table 2.2 displays the results of the model weights, calibration and cross validation skill scores, in the same format as described in the SST results section. Similar to the SST results, the temporal expansion series for mode 1 of Z_{500} turned out to be the predominant predictor driving the model. One hundred percent (100%) of the weight was applied to 500mb1 for both lead-times at all streamflow stations. Interestingly, we find that for both three and six month lead-times, the calibration skill values are all above +10% with substantial increase in skill for the three month OND(-1) lead-time. Likewise an improvement in cross validated skill is noticed for the OND(-1) lead-time over the JAS(-1) period. The cross-validated skill scores for the OND(-1) lead-time all exceed +10% whereas only one of the JAS(-1) skill scores exceed +5%. An explanation for these results will be examined in the discussion section. These results were similar to those of Grantz et al. [2005] in that an increase in skill was shown with decreasing lead-time when using the Z_{500} index as a predictor. Examples of poor and good exceedance probability forecasts utilizing Z_{500} are presented in Figure 2.5. Please refer to the discussion in the SST results section regarding the interpretation of poor and good exceedance probability forecast graphs.

DISCUSSION

The predefined climate index regions for the Niño 3.4, PDO and AMO lack the spatial-temporal relationship needed to produce skillful forecasts for the NPRB. In an attempt to find an ideal relationship, we expanded upon the methods of Grantz et al. [2005]. Through the use of a more powerful spatial-temporal analysis (SVD) we were able to locate “significant regions” of

SST and Z_{500} regions that tele-connected with the streamflow stations in the NPRB. The correlation values resulting from the SVD analysis, for each predictor, are displayed in Table 2.1. The SST "significant region" determined in this study was similar to that identified by Wang and Ting [2000], Tootle and Piechota [2006] and Grantz et al. [2005]. The unique aspect about the NPRB is that no significant SST regions were identified in the vicinity of the traditional ENSO belt (equatorial Pacific Ocean region). The predominant "significant region" identified for SSTs in this study was located approximately 20°W and 25° N of the Niño 3.4 region. Likewise, no significant regions were identified in the neighborhood of the typical PDO region. These findings verify the initial analysis which resulted in poor correlation values between the Nino 3.4, PDO and NPRB streamflow stations.

As a result of the stronger correlation values between NPRB streamflow stations and the AMO index in the preliminary analysis, the east longitudinal boundary was extended in an attempt to capture more Atlantic Ocean SST variability. The majority of the Atlantic Ocean SSTs displayed a significant relationship to NPRB streamflow (Figure 2.2), with a region off the coast of Africa displaying the highest significance. The region off the coast of Africa is similar to a region found in Tootle and Piechota [2006]. These findings reinforce the stronger correlation of the AMO index.

The significant region for Z_{500} (northwest/north central U.S.) was similar to the location found by Grantz et al. [2005]. There is a long history of the relationship between SSTs and streamflow forecasting but Grantz et al. [2005] and the work presented here examined the outcome of incorporating the 500 mbar geopotential height. Z_{500} is approximately 18,000 feet above sea level and has been linked to various climate processes. In mid-latitudes, Z_{500} transitions rapidly from large to low values across a circumpolar jet stream. A jet stream (fast flowing narrow currents of air) is located where the geopotential height contours are closest together (changing in height most rapidly). This jet stream consists of a series of transient troughs and ridges, which are the upper air counterparts of surface cyclones and anticyclones. The relatively shorter wave troughs in the jet stream are usually associated with surface cyclones and precipitation. Especially in winter, precipitation is strongly modulated by Z_{500}, and the deeper the short-wave trough or the stronger the jet, the more intense the surface cyclone and the heavier the precipitation. The precipitation is concentrated in frontal disturbances located just downstream of a Z_{500} trough. In the NPRB, most of that precipitation in winter falls as snow on the mountain ranges flanking the south and west sides of the upper NPRB. The general pattern of the polar jet stream over the United States in winter is such that it comes down from the coast of Alaska, just south of Anchorage, and then moves laterally from northwest to southeast across the northern tier of the continental United States. For regions that are typically equatorward of the jet, such as California and possibly also the upper NPRB, an anomalous southward excursion of the jet on average, over the course of a winter, should imply more trough passages and thus more precipitation. Places typically poleward of the jet, such as Fairbanks, Alaska, tend to be wetter when the jet is anomalously far north, i.e. when Z_{500} is anomalously high [B. Geerts, personal communication, 3/10/2008]. Grantz et al. [2005] explained that the Z_{500} and the wind vectors associated with the Z_{500} troughs and ridges drive winter precipitation over west central Nevada. These findings suggest that the winter weather in the west central U.S. is predominately driven by the location and magnitude of wind vectors (i.e., jet streams). Meteorological analyses examining the relationship between the jet stream, and pressure troughs and ridges suggest that precipitation responds immediately to Z_{500}. The jet stream and its wave train are very transient (e.g., a trough and its associated frontal precipitation may pass an area in less than a day). [B. Geerts, personal communication, 3/10/2008]. This concept of immediate response raises the question of how geopotential height index values can be incorporated into long lead-time forecasts.

The results of this study as well as those of Grantz et al. [2005] imply that an improved skill of streamflow forecasting is achieved at shorter lead-times. Since precipitation is an immediate response to geopotential heights it seems logical to conclude that there is no lag time between precipitation and the geopotential height index. Rather the geopotential heights are responsible for wintertime precipitation (falling as snow in the NPRB) when it is actually occurring (ONDJFM) and the three month lead-time is actually the typical time between when the snowfalls and the snow melts. We see a strong skill associated with the forecast utilizing OND(-1) geopotential heights because during those months the 500 mbar geopotential height index values are immediately driving the snowfall which settles, compacts and then begins melting several months later and is the prominent source of streamflow volume. Similar logic can be applied to the JAS(-1) time period. In mountainous regions, some precipitation may fall as snowfall but a substantial portion may still be falling in the form of rain due to the warmer temperatures of July, August and September. Due to the precipitation falling as rain and not snow, it is not accumulating as snowpack (which melts several months later and contributes to AMJJ streamflow) and therefore is not recognized as a skillful predictor in the model. Another question might be raised as to why not just use the actual snowpack amounts as measured at snow telemetry sites as opposed to incorporating Z_{500}.

The Natural Resource Conservation Service (NRCS) currently operates SNOTEL (snow water equivalent telemetry sites) throughout the west. However, January 1st data is only available back into the mid 1980's when most sites transferred from snowcourse sites to automated telemetry sites. Prior to the mid 1980's actual snowpack depth was only available for the months of March, April and May. The work of Moser et al. [2008] concludes a strong correlation between streamflow and snow water equivalent recorded by SNOTEL sites in the NPRB mountainous headwater regions. The results of this study suggest that Z_{500} index values can be a skillful predictor of winter precipitation and thus spring streamflow, especially in mountainous NBRB regions where the precipitation falls as snow. Therefore, if the 500 mbar geopotential height index values can be used as predictors of snowfall it can be concluded that for the NPRB this snowfall would result in AMJJ streamflow volumes.

CONCLUSION

A method for developing spatial-temporal relationships between large scale oceanic-atmospheric influences and incorporating those relationships into the development of exceedance probability forecasts for the North Platte River was performed. The North Platte River Basin is in a challenging location in terms of predefined climate index signals. The correlation between North Platte River streamflow volumes and the predefined Niño 3.4, PDO and AMO climate indices were found, in general, to be insignificant, thus creating the need to locate significant regions of oceanic-atmospheric variability. SVD was used to identify significant (>90%) spatial-temporal regions of SST and Z_{500} such that temporal expansion series (1st mode) found could be used to generate exceedance probability forecasts. Due to the continuous nature of the exceedance probability forecast, it is especially useful because it allows the forecast user to assess the forecasted amount of streamflow at different levels of risk. The forecast model was applied at two lead-times, three month—OND(-1) and six month—JAS(-1). The results of the modeling process reveal that SSTs are a skillful six month lead-time predictor whereas Z_{500} produce more skillful three month lead-time forecasts. Various years were selected to provide examples of good (high cross validated LEPS skill score) and poor forecasts. Over the 57 years used in this analysis, more good forecasts were developed versus poor forecasts, thus indicating that large scale oceanic-atmospheric climate variability is applicable to generating skillful long lead-time forecasts. The significant contribution of this work was the application of singular value decomposition techniques to identify predictors to be utilized in long lead-time streamflow forecasting models.

LITERATURE CITED

Blackmon, M. L. (1976).A climatological spectral study of the 500 mb geopotential height of the northern hemisphere. *Journal of the Atmospheric Sciences*. 33, 1607-1623.

Blackmon, M. L., Wallace, J. M., Lau, N. C., & Mullen, S. L. (1977). An observational study of the northern hemisphere wintertime circulation. *Journal of the Atmospheric Sciences*, 34, 1040-1053.

Bretherton, C.S., C. Smith, and J.M. Wallace (1992). An Intercomparison of Methods for Finding Coupled Patterns in Climate Data. *Journal of Climate*, 5, 541-560.

Cayan, D.R., and D.H. Peterson (1989). The influence of North Pacific atmospheric circulation on streamflow in the west. Aspects of Climate Variability in the Pacific and the Western Americas, *American Geophysical Union*, Geophysical Monograph Series, 55, 375-397.

Cayan, D.R., and R.H. Webb (1992). El Niño/Southern Oscillation and streamflow in the western United States. *El Niño: Historical and Paleoclimatic Aspects of the Southern Oscillation*. Cambridge University Press, New York, NY.

Elsner, J.B., and C. P. Schmertmann (1994). Assessing Forecast Skill through Cross Validation. and Forecasting 9:619-624.

Enfield, D.B., A.M. Mestas-Nuñez and P.J. Trimble (2001). The Atlantic multidecadal oscillation and its relation to rainfall and river flows in the continental U.S. *Geophysical Research Letters*, 28(10), 2077-2080.

Geerts, B. is an Associate Professor in the Department of Atmospheric Sciences at the University of Wyoming.

Grantz, K., Rajagopalan, B., Clark, M., & Zagona, E. (2005). A technique for incorporating large-scale climate information in basin-scale ensemble streamflow forecasts. *Water Resources Research*, *41*, W10410.

Hare, S., and N. Mantua (2000), Empirical evidence for North Pacific regime shifts in 1977 and 1989, *Prog. Oceanogr*., 47, 103– 145.

Hunter, T., Tootle, G., & Piechota, T. (2006). Oceanic-atmospheric variability and western U.S. snowfall. *Geophysical Research Letters*, *33*, L13706, doi:10.1029/2006GL026600.

Kahya, E., and J.A. Dracup (1993). U.S. streamflow patterns in relation to the El Niño / Southern Oscillation. *Water Resources Research*, 29(8), 2491-2503.

Kahya, E., and J.A. Dracup (1994a). The influences of Type 1 El Niño and La Niña Events on streamflows in the Pacific Southwest of the United States. *Journal of Climate*, 7(6), 965-976.

Kahya, E., and J.A. Dracup (1994b). The relationships between U.S. Streamflow and La Niña events. *Water Resources Research*, 30(7), 2133-2141.

Kalnay, E., et al. (1996). The NCEP/NCAR Reanalysis 40-year Project. *Bull. Amer. Meteor. Soc*., 77, 437-471.

Lall, U. (1995). Recent advances in non-parametric function estimation; Hydrologic applications, *U.S. Natl. Rep. Int. Union Geod. Geophys. 1991-1994, Rev. Geophys., 33,* 1093-1102.

Lall, U., and A. Sharma (1996). A nearest neighbor bootstrap for resampling hydrologic time series. *Water Resources Research,*32, 679-693.

Mantua, N.J., S.R. Hare, Y. Zhang, J.M. Wallace, and R.C. Francis (1997). A Pacific interdecadal climate oscillation with impacts on salmon production. *Bulletin of the American Meteorological Society*, 78, 1069-1079.

Mantua, N.J. and S.R. Hare (2002). The Pacific Decadal Oscillation. *Journal of Oceanography*, 59(1), 35-44.

Maurer, E.P., D.P. Lettenmaier and N.J. Mantua (2004). Variability and potential sources of predictability of North American runoff. *Water Resources Research*, 40(12), W09306.

McCabe, G.J., M.A. Palecki and J.L. Betancourt (2004). Pacific and Atlantic Ocean influences on multidecadal drought frequency in the United States. *PNAS*, 101(12), 4136-4141.

Michaelsen, J. (1987). Cross-Validation in Statistical Climate Forecast Models. *Journal of Climate and Applied Meteorology* 26:1589-1600.

Moser, C., T. Soukup, G. Tootle and T. Piechota (2009). Incorporating Antecendent Soil Moisture into Streamflow Forecasting - North Platte River Basin, Wyoming (in prep).

Natural Resources Conservation Service. *Water Supply Forecasting, A Short Primer*. Retrieved January 15, 2008, Web site: http://www.wcc.nrcs.usda.gov/factpub/wsf_primer.html

Newman, M. and P.D. Sardeshmukh (1995). A caveat concerning singular value decomposition. *Journal of Climate*, 8, 352-360.

North Platte River Basin (Overview) HUC# 101800. Retrieved March 21, 2008, from Wyoming State Water Plan Web site: http://waterplan.state.wy.us/sdi/NP/NP-over.html

Piechota, T.C., and J.A. Dracup (1999). Long Range Streamflow Forecasting Using El Niño-Southern Oscillation Indicators. *Journal of Hydrologic Engineering*, 4(2), 144-151.

Piechota T.C., and, F.H.S. Chiew, J.A. Dracup, and T.A. McMahon (2001). Development of Exceedance Probability Streamflow Forecast. *Journal of Hydrologic Engineering* 6(1):20-28.

Piechota T.C., and J.A. Dracup, F.H.S. Chiew, and T.A. McMahon (1998). Seasonal Streamflow Forecasting in Eastern Australia and the El Niño-Southern Oscillation. *Journal of Water Resources Research* 34(11):3035-3044.

Philander, S.G. (1990). *El Niño, La Niña and the Southern Oscillation*. Academic Press, Inc., San Diego, CA.

Potts, J.M., and C.K. Folland, I.T. Jolliffe, and D. Sexton (1996). Revised "LEPS" Scores for Assessing Climate Model Simulations and Long-Range Forecasts. *Journal of Climate* 9:34-53.

Rajagopalan, B., and U. Lall (1999). A k-nearest-neighbor simulator for daily precipitation and other weather variables. *Water Resources Research*, 35, 3089-3101.

Rajagopalan B., E. Cook, U. Lall, and B.K. Ray (2000). Spatiotemporal variability of ENSO and SST teleconnections to summer drought over the United States during the twentieth century. *Journal of Climate*, 13, 4244-4255

Reclamation (U.S. Department of the Interior, Bureau of Reclamation) 2007. Draft Environmental Impact Statement, Colorado River Interim Guidelines for Lower Basin Shortages and Coordinated Operations for Lake Powell and Lake Mead.

Rogers, J.C. and J.S.M. Coleman (2003). Interactions between the Atlantic Multidecadal Oscillation, El Niño/La Niña, and the PNA in winter Mississippi Valley stream flow. *Geophysical Research Letters*, 30(10), 25, 1-4.

Serreze, M. C., Clark, M. P., McGinnis, D. L., & Robinson, D. A. (1998). Characteristics of snowfall over the eastern half of the United States and relationships with principal modes of low-frequency atmospheric variability. *Journal of Climate*, *11*, 234-250.

Silverman, B.W. (1986) . Density Estimation for Statistics and Data Analysis, Chapman and Hall, New York.

Smith, T.M., and R.W. Reynolds (2003). Extended Reconstruction of Global Sea Surface Temperatures Based on COADS Data (1854-1997). *Journal of Climate*, 16, 1495-1510.

Smith, T.M., and R.W. Reynolds (2004). Improved Extended Reconstruction of SST (1854-1997). *Journal of Climate*, 17, 2466-2477.

Souza Filho, F.A., and U. Lall (2003). Seasonal to interannual ensemble streamflow forecasts for Ceara, Brazil: Applications of multivariate, semiparametric algorithm. *Water Resources Research*, 39(11), 1307, doi: 10.1029/2002/WR001373

Tootle, G.A., and T.C. Piechota (2004). Suwannee River Long-Range Streamflow Forecasts based on Seasonal Climate Predictors. *Journal of the American Water Resources Association,* 40(2), 523-532.

Tootle, G. A., and T. C. Piechota (2006). Relationships between Pacific and Atlantic ocean sea surface temperatures and U.S. streamflow variability, *Water Resources Research*, 42, W07411.

Tootle, G. A., T. C. Piechota, and A. Singh (2005), Coupled oceanic-atmospheric variability and U.S. streamflow, *Water Resources Research*, 41, W12408, doi: 10.1029/2005WR004381.

Tootle, G.A., T.C. Piechota and F. Gutierrez (2008). The Relationships between Pacific and Atlantic Ocean Sea Surface Temperatures and Colombian Streamflow Variability. *Journal of Hydrology*, 349(3-4), 268-276.

Trenberth, K.E. (1997). The definition of El Niño. *Bulletin of the American Meteorological Society*, 78, 2271-2777.

United States Geological Survey, USGS Real-Time Water Data for USA . Retrieved November 17, 2007, from National Water Information System: Web Interface Web site: http://waterdata.usgs.gov/nwis/rt?

Uvo, C.B., C.A. Repelli, S.E. Zebiak, and Y. Kushnir (1998). The relationships between tropical Pacific and Atlantic SST and northeast Brazil monthly precipitation. *Journal of Climate*, 11, 551-562.

Wallace, J.M., D.S. Gutzler, and C.S. Bretheron (1992). Singular Value Decomposition of Wintertime Sea Surface Temperature and 500-mb Height Anomalies. *Journal of Climate*, 5, 561-576.

Wang, H. and M. Ting (2000). Covariabilities of winter U.S. precipitation and Pacific sea surface temperatures. *Journal of Climate*, 13, 3711-3719.

Ward, N.M., and K.K Folland (1991). Prediction of Seasonal Rainfall in the North Nordeste of Brazil using Eigenvectors of Sea-Surface Temperature. *International Journal of Climatology* 11:711-743.

Xoplaki, E., Luterbacher, J., Burkard, R., Patrikas, I., & Maheras, P. (2000). Connection between the large-scale 500 hPa geopotential height fields and precipitation over Greece during wintertime. *Climate Research*. *14*, 129-146.

TABLE AND FIGURE CAPTIONS

Table 2.1: Correlation table of current seasonal (spring-summer, AMJJ) streamflow (Q) and previous [JAS (-1) and OND(-1)] seasonal climate indices (Nino 3.4, PDO, AMO) and Temporal Expansion Series (1st, 2nd and 3rd modes) for SSTs[1,2,3] and Z500[1,2,3].

Table 2.2: Weighting and LEPS [Calibration (Cal) and Cross Validation (CV)] score skill table of current seasonal (spring-summer, AMJJ) streamflow (Q) and previous [JAS (-1) and OND(-1)] seasonal climate indices (Nino 3.4, PDO, AMO) and Temporal Expansion Series (1st, 2nd and 3rd modes) for SSTs[1,2,3] and Z500[1,2,3].

Figure 2.1: North Platte River Basin and USGS Streamflow Stations Location Map.

Figure 2.2: Heterogeneous correlation map showing significant [$|r| > 0.21$ for 90% ($p < 0.1$) significance threshold] SST regions as related to NPRB streamflow stations for JAS(-1) six month lead-time.

Figure 2.3: Examples of poor and good forecasts for JAS(-1) SSTs and individual streamflow stations.

Figure 2.4: Heterogeneous correlation map showing significant [$|r| > 0.21$ for 90% ($p < 0.1$) significance threshold] Z_{500} regions as related to NPRB streamflow stations for OND(-1) three month lead-time.

Figure 2.5: Examples of poor and good forecasts for OND Z_{500} index values and individual streamflow stations.

Table 2.1

JAS(-1)	Q1 (AMJJ)	Q2 (AMJJ)	Q3 (AMJJ)	Q4 (AMJJ)	OND(-1)	Q1 (AMJJ)	Q2 (AMJJ)	Q3 (AMJJ)	Q4 (AMJJ)
Nino 3.4	-0.03	-0.07	0.02	0.17	Nino 3.4	-0.04	-0.09	0	0.19
PDO	0.02	-0.03	-0.04	0.04	PDO	-0.12	-0.15	-0.15	-0.01
AMO	-0.24	-0.25	-0.27	-0.37	AMO	-0.17	-0.15	-0.16	-0.34
SST1	0.43	0.41	0.49	0.54	SST1	0.52	0.49	0.53	0.58
SST2	-0.09	-0.16	-0.06	0.25	SST2	-0.09	-0.16	-0.04	0.25
SST3	0.09	0.07	-0.17	0.03	SST3	0.17	-.06	-0.11	-0.00
500mb1	0.38	0.42	0.43	0.38	500mb1	0.52	0.53	0.56	0.45
500mb2	-0.05	-0.04	-0.06	0.16	500mb2	-0.02	-0.05	-0.06	0.16
500mb3	0.03	-0.10	0.06	0.00	500mb3	0.15	-0.11	-0.02	-0.02

Table 2.2

JAS(-1)	Q1 (AMJJ)	Q2 (AMJJ)	Q3 (AMJJ)	Q4 (AMJJ)	OND(-1)	Q1 (AMJJ)	Q2 (AMJJ)	Q3 (AMJJ)	Q4 (AMJJ)
Nino 3.4	0%	0%	0%	0%	Nino 3.4	33%	95%	77%	0%
PDO	0%	0%	0%	0%	PDO	0%	0%	3%	2%
AMO	100%	100%	100%	100%	AMO	67%	5%	20%	98%
Cal Skill	9.2%	11.6%	8.9%	13.8%	Cal Skill	5.0%	6.1%	5.2%	8.8%
CV Skill	***1.0%***	***0.7%***	***-1.4%***	***1.4%***	***CV Skill***	***-8.6%***	***-4.5%***	***-9.6%***	***-0.7%***
SST1	100%	100%	100%	100%	SST1	100%	100%	100%	100%
SST2	0%	0%	0%	0%	SST2	0%	0%	0%	0%
SST3	0%	0%	0%	0%	SST3	0%	0%	0%	0%
Cal Skill	16.4%	21.4%	18.2%	20.6%	Cal Skill	16.5%	21.4%	18.1%	16.6%
CV Skill	***7.3%***	***8.5%***	***8.1%***	***10.2%***	***CV Skill***	***2.9%***	***6.2%***	***5.7%***	***4.7%***
500mb1	100%	100%	100%	100%	500mb1	100%	100%	100%	100%
500mb2	0%	0%	0%	0%	500mb2	0%	0%	0%	0%
500mb3	0%	0%	0%	0%	500mb3	0%	0%	0%	0%
Cal Skill	16.7%	15.4%	15.3%	14.3%	Cal Skill	23.9%	25.1%	25.0%	20.3%
CV Skill	***3.6%***	***3.3%***	***5.7%***	***4.5%***	***CV Skill***	***12.8%***	***14.6%***	***13.7%***	***10.4%***

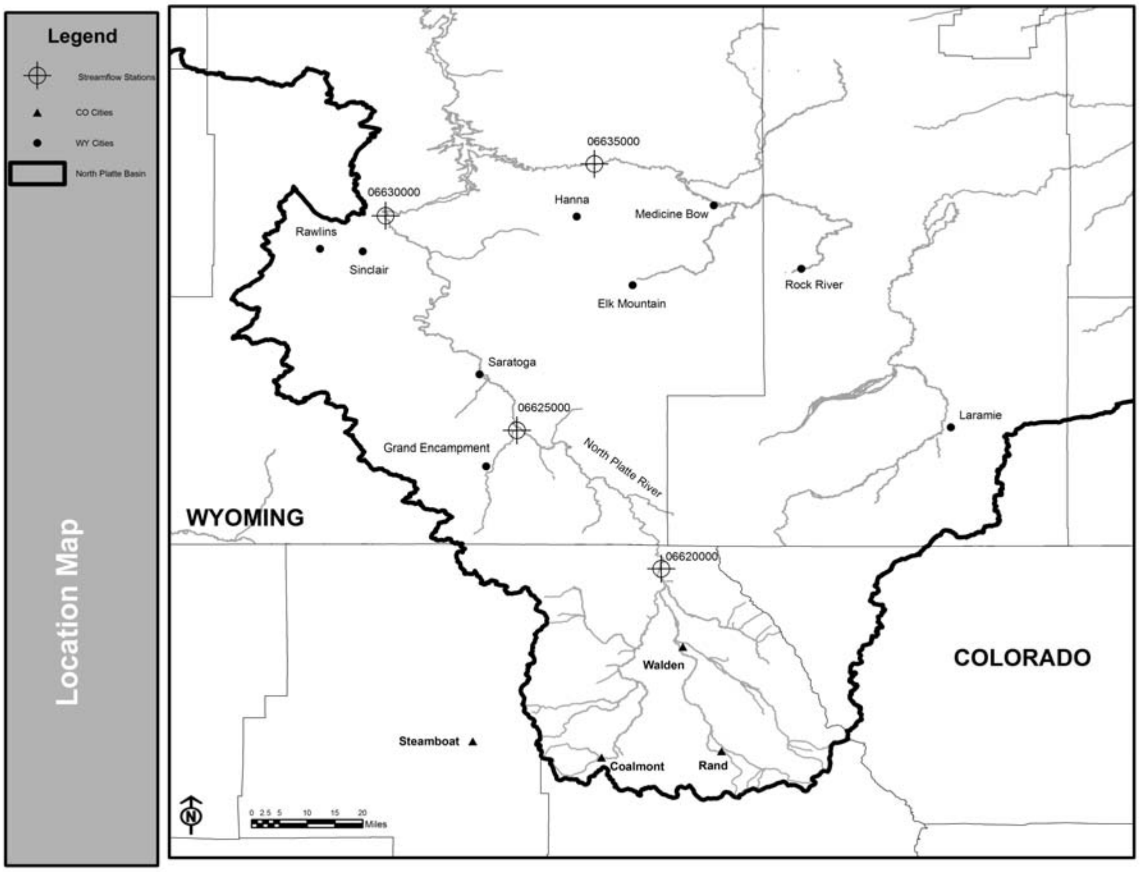
Legend
Streamflow Stations
CO Cities
WY Cities
North Platte Basin
Location Map
06635000
06630000
Hanna
Medicine Bow
Rawlins
Sinclair
Rock River
Elk Mountain
Saratoga
06625000
Grand Encampment
North Platte River
Laramie
WYOMING
06620000
Walden
COLORADO
Steamboat
Coalmont
Rand
0 2.5 5 10 15 20
Miles
N

Figure 2.1

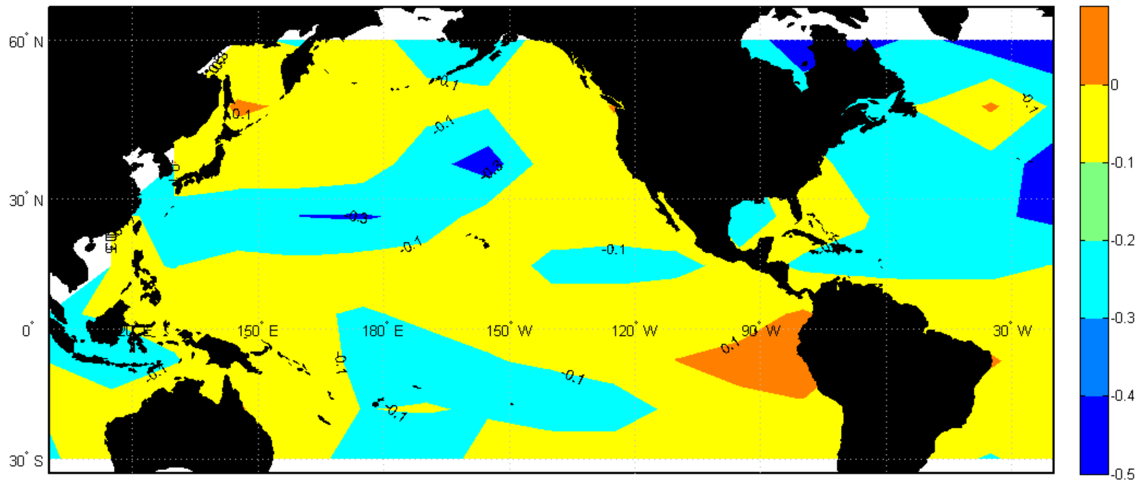

Figure 2.2

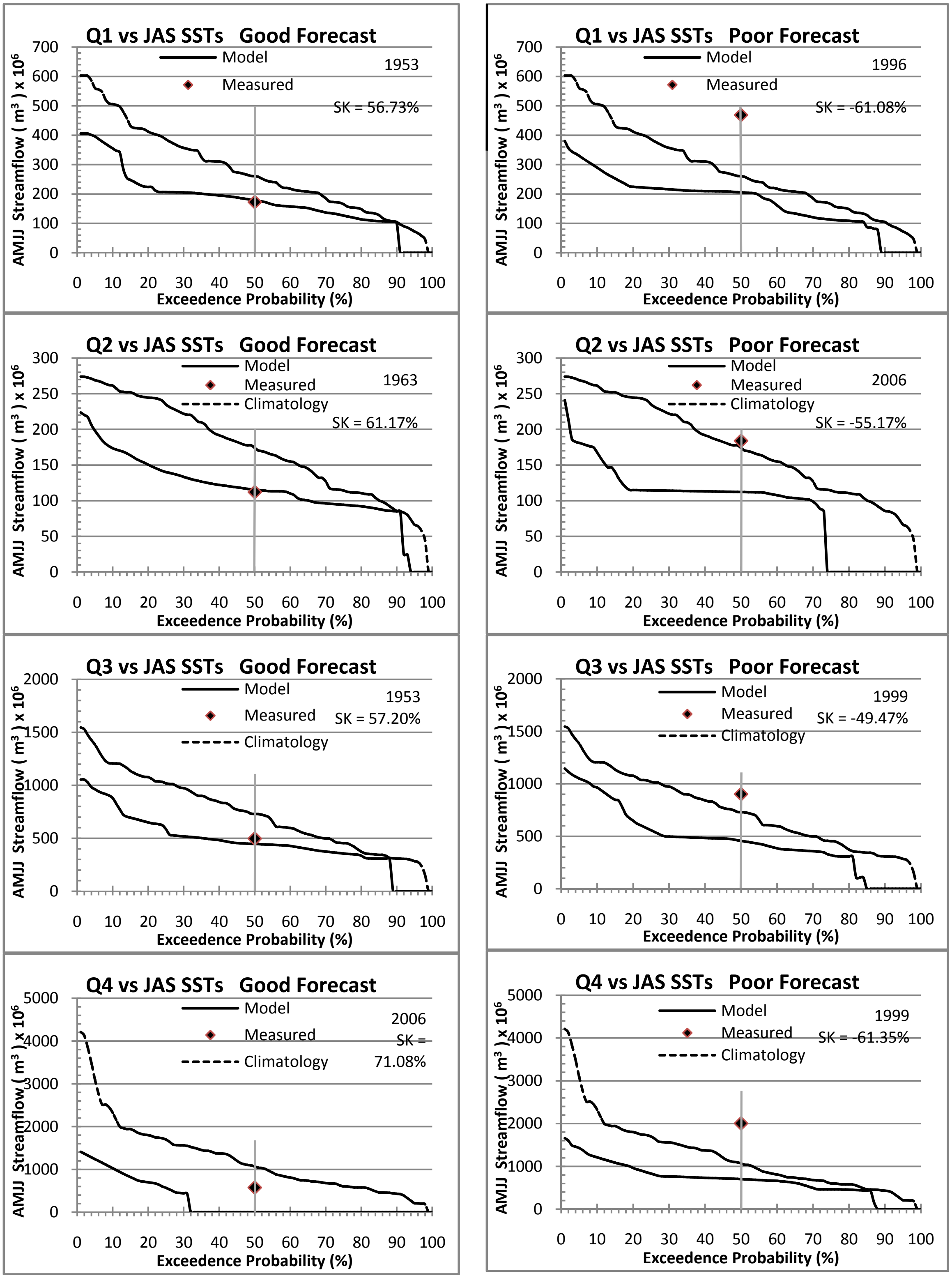
Q1 vs JAS SSTs Good Forecast
Model
Measured
1953
SK = 56.73%
Q1 vs JAS SSTs Poor Forecast
1996
SK = -61.08%
Q2 vs JAS SSTs Good Forecast
Climatology
1963
SK = 61.17%
Q2 vs JAS SSTs Poor Forecast
2006
SK = -55.17%
Q3 vs JAS SSTs Good Forecast
1953
SK = 57.20%
Q3 vs JAS SSTs Poor Forecast
1999
SK = -49.47%
Q4 vs JAS SSTs Good Forecast
2006
SK =
71.08%
Q4 vs JAS SSTs Poor Forecast
1999
SK = -61.35%
AMJJ Streamflow (m³) x 10⁶
Exceedence Probability (%)

Figure 2.3

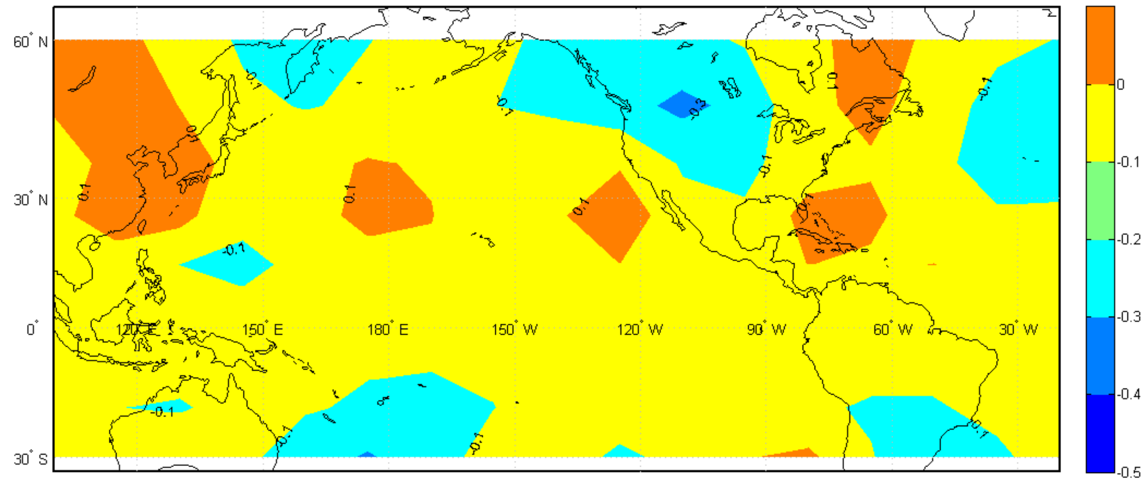
60° N
30° N
0°
30° S
120° E
150° E
180° E
150° W
120° W
90° W
60° W
30° W
0
-0.1
-0.2
-0.3
-0.4
-0.5

Figure 2.4

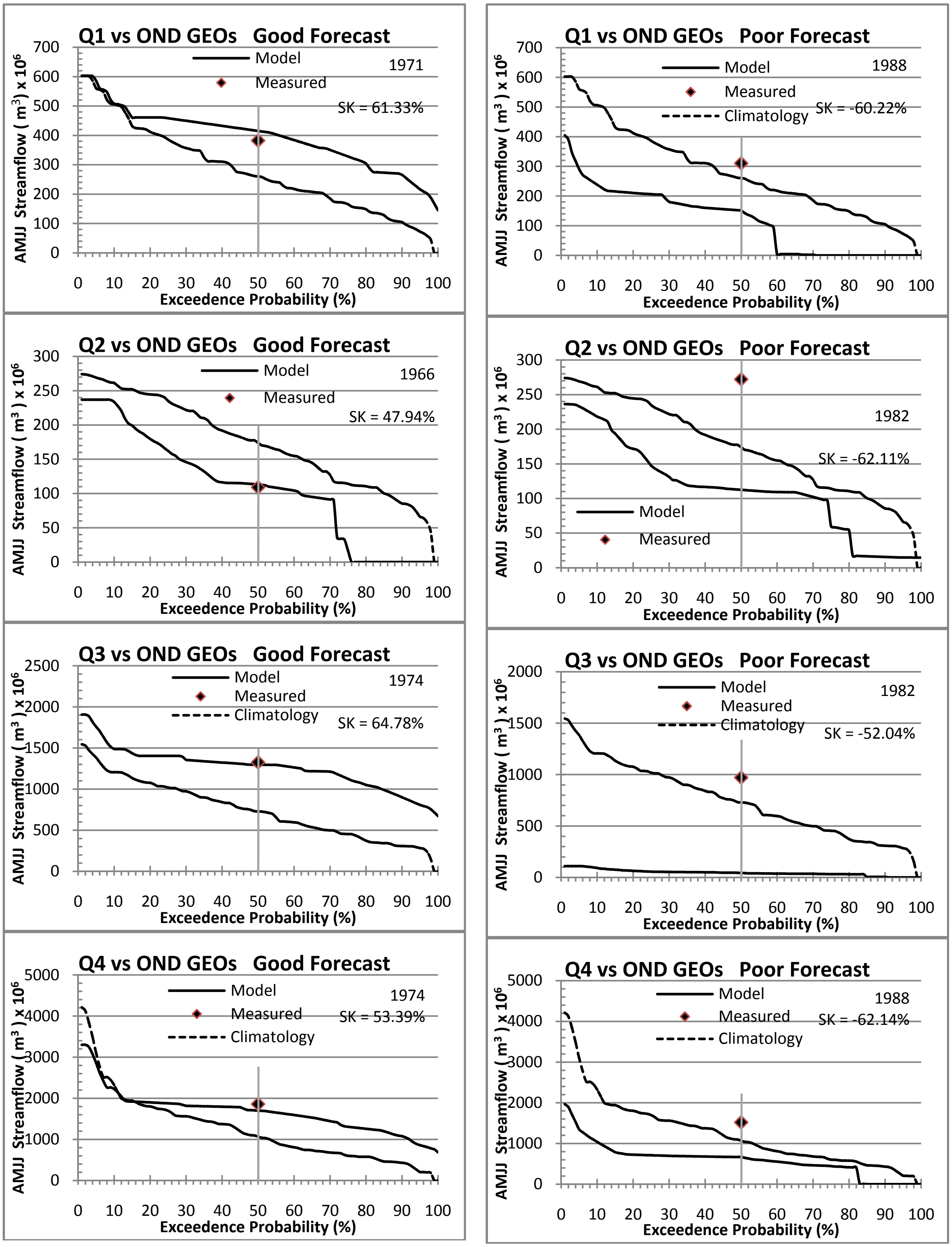
Q1 vs OND GEOs Good Forecast
Model
Measured
1971
SK = 61.33%
Q1 vs OND GEOs Poor Forecast
Model
Measured
Climatology
1988
SK = -60.22%
Q2 vs OND GEOs Good Forecast
Model
Measured
1966
SK = 47.94%
Q2 vs OND GEOs Poor Forecast
Model
Measured
1982
SK = -62.11%
Q3 vs OND GEOs Good Forecast
Model
Measured
Climatology
1974
SK = 64.78%
Q3 vs OND GEOs Poor Forecast
Model
Measured
Climatology
1982
SK = -52.04%
Q4 vs OND GEOs Good Forecast
Model
Measured
Climatology
1974
SK = 53.39%
Q4 vs OND GEOs Poor Forecast
Model
Measured
Climatology
1988
SK = -62.14%
AMJJ Streamflow (m³) x 10⁶
Exceedence Probability (%)

Figure 2.5